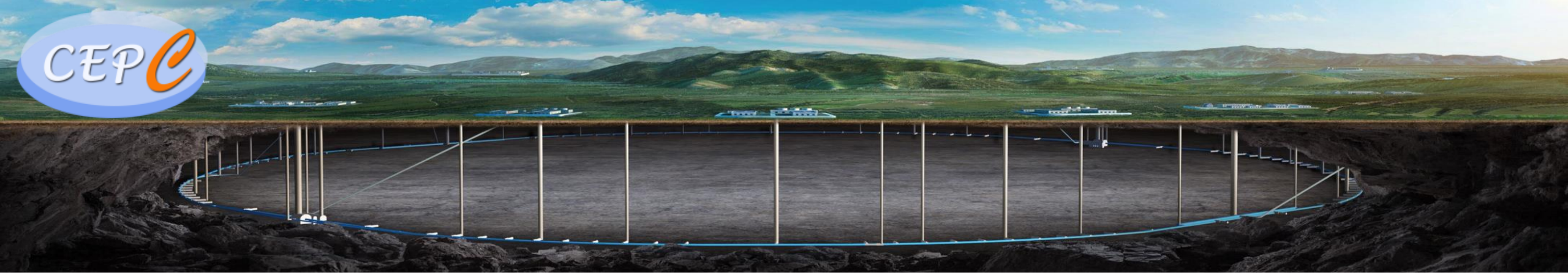

Feedback of 2025 IDRC Review Report

中国科学院高能物理研究所
Institute of High Energy Physics
Chinese Academy of Sciences

Machine Detector Interface

Findings

- A layout of the interaction region—including the anti-solenoid, final focus quadrupoles, IP beam pipe, and Luminosity Monitor—has been presented. Although not yet final, it is sufficiently advanced to proceed with detailed component design.
- The Be beam pipe has an inner diameter of 10 mm and a length of 220 mm. It consists of an inner Be layer 0.2 mm thick and an outer Be layer 0.15 mm thick, separated by a 0.2 mm gap, which seems quite aggressive. The default coolant is water, with paraffin as a backup. The cooling technology is well-established, and the cost estimates are considered reliable. The coolant flow remains in the stable laminar regime. Mechanical analyses for cantilever support during installation have been performed, and no issues have been found. With an inlet water temperature of 15° C, the Be pipe temperature remains below 20° C, which is within acceptable limits.
- Beam background sources—including synchrotron radiation (SR) photons, pairs, and off-energy particles—have been studied in detail, along with other minor contributions. For SR photons, important interactions such as the photoelectric effect and Rayleigh scattering have been simulated. It was found critically important to employ high-Z SR masks to protect the IP beam pipe region. Pair backgrounds are mitigated by designing the IP beam pipe to stay outside the high- density region. The hit rate on the first layer of the vertex detector (VTX) is estimated to be around 1 hit per cm^2 per bunch crossing. Backgrounds from off-energy particles are suppressed by placing collimators at strategic points around the ring and heavy metal masks near the IP to absorb secondary showers.
- Experience from BESIII was presented, showing that real background levels were about 1/5 of those predicted by simulation.
- An updated design of the LumiCal, using a silicon detector and LYSO crystals for pile-up event veto, is included in the Reference TDR. Mechanical design and optimization are complete, and construction of a large prototype is planned for the EDR phase. The selected technology appears feasible, although achieving the required luminosity precision will demand electron impact position measurements at the level of better than ten microns.

Comments

- From the presentations and draft Ref-TDR, it is unclear whether a gold (Au) coating is applied to the inside of the Be beam pipe, and if so, what thickness is used. Further study on this issue may be necessary.
- Answer: The 5um Au coating is implemented, as indicated in Ref-TDR MDI Chapter: “In addition, a 5 μm thick layer of gold is coated on the inner surface of the central beryllium pipe to prevent SR photons entering the detector.”
- The current SR mask configurations require further study. In particular, changes in beam or bit— such as during commissioning— must be considered to ensure continued protection of the Be beam pipe region.
- Answer: Currently, only the ideal beam has been studied. The changes in beam orbit will be studied in future together with accelerator colleagues to figure out the working scenarios and the parameters.
- While heavy metal masks can effectively reduce backgrounds from off-energy particles, they may also generate secondary backgrounds. This study suggests the effect is moderate, but further investigation is needed, especially concerning the tungsten (W) masks near the IP.
- Answer: The secondaries has been studied. We also realize that the SR masks in the -1.9m may also increase the other sources of beam induced backgrounds. We are optimizing our design of the SR masks, by introducing some dedicated SR collimators relatively far away from the IP, the decrease the height of the SR mask to mitigate the secondaries introduced by it. These work is still on going.

Comments

- The discrepancy between real background measurements and simulations observed at BESIII is a significant concern. Although the energy scales differ between BESIII and CEPC, understanding this discrepancy is critical for evaluating the reliability of CEPC background predictions.
- Answer: The previous study already decreased the discrepancy as shown in the text, and we will perform more dedicated study in future when we have machine times.
- Although background rates (after shielding) are presented, detailed histograms and numerical data characterizing these backgrounds (e.g., energy spectra, multiplicity, polar and azimuthal angle distributions) are often missing. Such information is essential to assess the impact on the entire apparatus, particularly on the first layers of the vertex detector and LumiCal.
- Answer: We have those information, and all these information have been given to the subdetector designers as indicated in MDI Chapter LINE 462-469. Further optimization for LumiCal is also needed, and the study taking the beam induced background at LumiCal is still on going.

Recommendations

- Conduct studies to finalize the decision on the Au coating inside the Be beam pipe, including its thickness and the possibility of omitting it.
- Answer: The 5um Au coating is implemented, as indicated in Ref-TDR MDI Chapter: “In addition, a 5 μm thick layer of gold is coated on the inner surface of the central beryllium pipe to prevent SR photons entering the detector.”
- Continue detailed studies of SR mask configurations and materials, considering the effects of beam orbit steering in collaboration with the accelerator group.
- Answer: Currently, only the ideal beam has been studied. The changes in beam orbit will be studied in future together with our accelerator colleagues when they have the results of the orbit corrections and the parameters and designs used for the commissioning phase.
- Further investigate the role of heavy metal masks in absorbing particle backgrounds, including the possibility of operating without them.
- Answer: The secondaries has been studied. We also realize that the SR masks in the -1.9m may also increase the other sources of beam induced backgrounds. We are optimizing our design of the SR masks, by introducing some dedicated SR collimators relatively far away from the IP, the decrease the height of the SR mask to mitigate the secondaries introduced by it. These work is still on going.

Recommendations

- Pursue deeper studies of BESIII backgrounds to understand the discrepancy between simulation and data.
- Answer: The previous study already decreased the discrepancy as indicated in MDI Chapter: ”Such discrepancy was mainly due to the incomplete particle tracking and insufficiently modeled interactions involving complex components in IR in the simulation and was already decreased from more than 10^4 to current level by the improving of the geometry and adding the study on tip-scattering on the collimators”, and we will perform more dedicated study in future. We are working on the analysis of the data currently taking from BEPCIIU, and plan to perform this years dedicated beam induced backgrounds study and experiments at BEPCII when possible.
- Continue dedicated studies on LumiCal readout electronics at high rates, followed by beam tests with detector prototypes at later stages.
- Study the effects of beam backgrounds on LumiCal reconstruction for realistic configurations.
- Answer: The shielding optimization and further mitigation of the beam induced background at LumiCal is still ongoing. Current beam induced background level is high at LumiCal, therefore the dedicated optimization must be performed to control the level and let the LumiCal works better. The data rate due to the beam induced backgrounds are already considered when design the electronics of the LumiCal. Such studies are ongoing at the same time to give us an idea how the situation would be.

Vertex Detector

Findings

- The design and technology choice for the vertex detector is highly ambitious and at the forefront of technological innovation. The baseline option—thin, bendable silicon CMOS sensors that can be stitched together to create a large, lightweight vertex detector—is certainly a very challenging yet promising approach. The backup solution, which also employs thin CMOS sensors mounted on ladders, remains technologically advanced. The project has made significant progress since the last review.
- The vertex detector is expected to operate for 10 years during Higgs and low-luminosity Z running, after which it will need to be replaced for high-luminosity Z, WW, and $t\bar{t}$ operations. The ability to run at high-luminosity Z mode imposes additional demands on an already extremely challenging design (e.g., larger data rate capabilities, shorter charge collection times, lower noise, and tighter power consumption constraints).
- There are several major challenges for the vertex detector. Achieving the desired position resolution has been demonstrated with the TaichuPix-3 chip in TJ180 nm technology. However, this process has limitations, particularly its high-power consumption (>100 mW/cm²), which is too high for air cooling. Transitioning to the TPSCo65 process is a way forward, reducing power consumption to approximately 40 mW/cm². The required position resolution and uniform hit efficiency have already been demonstrated in this new process.
- The real challenge now lies in the development of large-area stitched sensors of ~40 μm thickness that can be bent to radii as small as 11 mm, achieving a material budget of just 0.06% X_0. Successful bending of dummy 40 μm wafers has been demonstrated, but bending fully processed wafers (including metal layers for data and power lines) remains to be achieved. Securing access to TPSCo65 technology, including a modified process optimized for particle detection, is crucial. An alternative approach under early exploration is the HLMC 55 nm technology, although it has yet to be demonstrated.
- The mechanical design is quite advanced for this stage, with many demonstrators and mock-up parts already tested, including a full ladder demonstrator. The simulations shown for mechanical and thermal performance, efficiency coverage, and background hit rates are detailed and of high quality. The impact of background hit rates on physics performance has been found to be negligible. The planned laser alignment system is a very positive development, but its effective operation must still be demonstrated.
- The fifth double layer of the vertex detector employs a more conventional ladder design, achieving approximately 0.25% X_0. At the larger radius of the fifth layer, this becomes necessary but also requires parallel development. Importantly, this ladder design offers a reliable fallback option in case insurmountable problems arise with the stitched sensor technology for the inner layers.
- However, adopting this backup would come at the cost of a slightly higher material budget, and thus a somewhat degraded p_t resolution at lower energies.

Comments

- **The chapter in the TDR is very long and detailed. In sections covering previously published R&D, the level of detail could be reduced.** However, we found it very positive that past efforts from various groups were acknowledged, and that valuable experience and knowledge have been incorporated into the current vertex detector design.
  - This section has been reduced from ~70 pages to 40 pages
- Although pursuing the HLMC 55 nm process could dilute focus and resources, it remains a worthwhile avenue, especially if difficulties arise in securing access to TPSCo65.
- While the mechanical design, simulations, and testing are advanced for this stage, maintaining mechanical stability and achieving efficient cooling remain significant challenges.
- The foreseen cost of sensors (~4.0 MCHF) appears reasonable. The relatively higher cost per unit area compared to other silicon detectors likely reflects the fact that the baseline sensor producer is not domestic.
- The estimated costs for mechanics, electronics, and the alignment system are of the correct order of magnitude but constitute only a fraction of the sensor cost

Recommendations

•Re-evaluate the required performance specifications, focusing on operation during ZH and low-luminosity Z runs over the first 10 years.

•Answer: the new result of hit rate with latest simulation is updated in Sec 4.1.3.

•We reiterate our previous recommendation to expand the current manpower dedicated to design and R&D efforts. A close collaboration with ALICE-ITS3 on stitched sensor development is strongly encouraged.

•Answer: synergy with sensor development in future ALICE3 upgrade is expected.

•Explore constructing a mock-up with dummy heaters for thermal performance tests, to be used also for simulation validation.

•Answer: has added this suggestion into future plan section in vertex chapter sec. 4.8. 'The plan begins with exploring the construction of a mock-up featuring dummy heaters for thermal performance testing. Results will also validate thermal simulation models.'

•While pixel functionalities are similar for the ladder and stitched sensor options, significant differences in chip-to-chip (RSU-to-RSU) connectivity could impact performance. Address potential challenges (e.g., power and data distribution across large, stitched sensors) as early as possible through simulation studies

•Answer: will perform simulation on stitching design when we are about to tape out the next version of sensor by the end of 2025. Most of this potential challenges can be simulated with design kits when the stitching design is in shape.

Inner Tracker (ITK)

Findings

- The Inner Tracker (ITK) of the CEPC silicon tracking system adopts a baseline technology based on HV-CMOS monolithic active pixel sensors (SMIC 55), offering excellent spatial resolution (pixel size: 34 μm × 150 μm), moderate time resolution (3–5 ns), and low material per layer (<1% X_0). As an alternative for the endcap, a HV-CMOS strip sensor technology is also under development.
- Since the last review in October 2024, the project has made notable progress in ASIC development. The COFFEE3 chip (SMIC 55 nm)—the second-generation HV-CMOS prototype— was successfully submitted for fabrication in January 2025 and is expected to be delivered for testing in May 2025. COFFEE3 integrates two readout architectures, supports in-pixel time stamping, and includes significant improvements in power optimization and data-driven readout. In parallel, the CSC1 chip, which integrates a passive CMOS strip sensor and an analog front-end placed in the periphery (CMSC 180 nm process), is scheduled for tape-out in April 2025. Together, these developments demonstrate strong and steady progress in the ITK technology program.
- Significant system-level advancements have also been achieved, particularly in mechanical design, cooling, and thermal management. The ITK now incorporates a well-defined multi-loop water-cooling system capable of maintaining stable operation at a power density of ~200 mW/cm², with thermal gradients controlled below 4° C. Updated mechanical simulations confirm the structural integrity of staves and validate the mechanical design for integration and prototyping.

Comments

- The alternative ITK endcap technology based on CMOS strips, while offering slightly better intrinsic spatial resolution (~4 μm), presents greater challenges compared to the HVCMOS pixel baseline. Achieving 3D tracking requires stereo configurations, increasing the material budget and mechanical complexity. Furthermore, the integration of a CMOS readout circuit in the strip sensor periphery, although innovative, may introduce additional design and integration risks.

- The COFFEE3 chip successfully consolidates the sensor, analog front-end, coarse-fine TDC for time-of-arrival and time-over-threshold measurements, and data-driven digital readout into a single device. Achieving these capabilities within a power density of ~200 mW/cm^2 is an impressive technical goal. A successful validation of COFFEE3 would represent a major milestone, demonstrating the technological feasibility of the CEPC ITK concept

Recommendations

- Given the limited resources available for R&D and the increased complexity associated with the CMOS strip-based solution for the ITK endcap, we recommend a careful evaluation of the merit and timing of continuing this development. The CMOS strip approach remains a promising technological direction; however, it may be appropriate to continue work at a lower priority to preserve long-term potential, while focusing current resources on advancing the baseline HV-CMOS pixel system.

We thank the Referee for the comment. In our previous Ref-TDR draft, the CMOS strip was presented as a backup or alternative approach with low R&D priority. Following the Referee's comment , we have removed all content related to CMOS strip from the current Ref-TDR to better focus on HV-CMOS baseline.

- We strongly encourage prioritizing the COFFEE3 validation campaign. As a comprehensive integration of position sensing and timing capabilities within a monolithic HV-CMOS technology, successful testing of COFFEE3 would constitute a critical milestone for the CEPC silicon tracking system, helping to de-risk the ITK concept and validate the soundness of the baseline detector design.

The latest COFFEE3 sensor was received at the end of May, and the sensor test campaign was lunched immediately upon receipt. The test setup is fully prepared, and testing is currently underway. We are committed to completing the critical validation promptly, as it represents one of the most important milestones for the ITK.

Recommendations

COFFEE3 incorporates two readout architectures, both featuring nearly a complete ASIC readout framework. This solution can be extended to final chip.

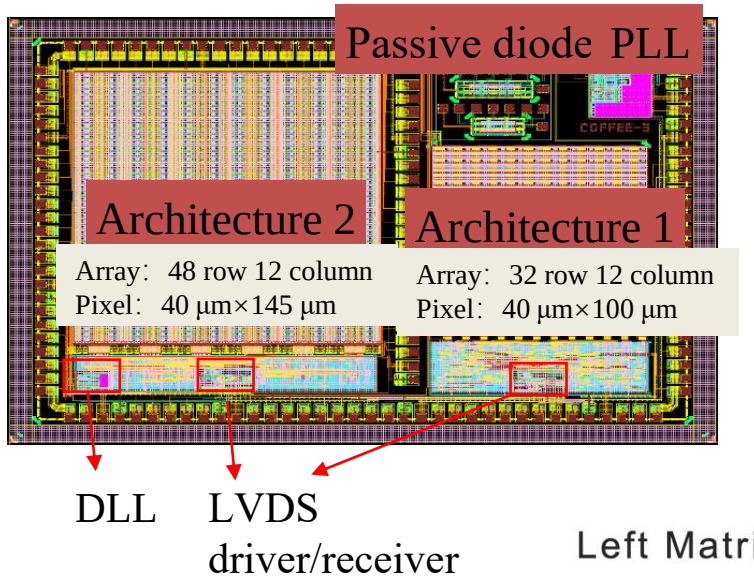

- **Architecture 1:** An optimized design framework based on the current process conditions (Triple-well process);
- **Architecture 2:** An improved solution that requires process modification (Deep P-well required) to fully utilize the advantages of the 55 nm process node.

Caribou DAQ at IHEP

- both ZC706 and ZCU102 running fine with CaR boards

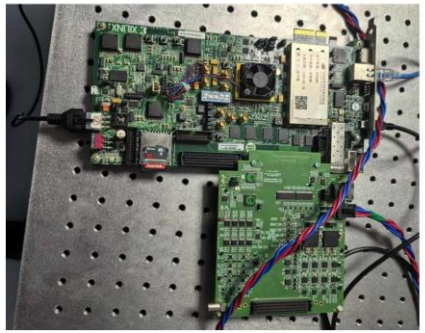

Left Matrix Test Board

- TB v1.2 Board in production, will arrive early next week
- COFFEE3 left matrix test will starting immediately

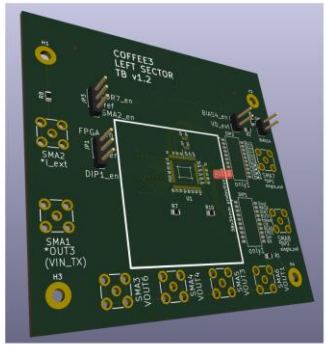

PLL (and IV) Test Board

- Mostly for PLL block only

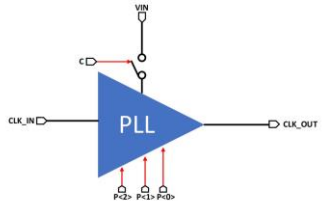

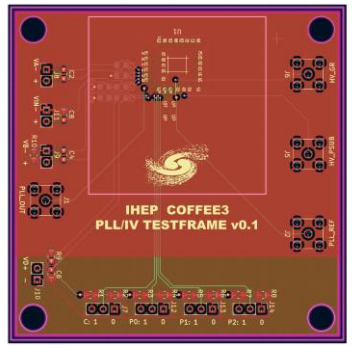

- SPI config between the FPGA and the CMOS matrix EOC
- power supply from Caribou DAQ
- reference voltage/current from Caribout to CMOS matrix
- 4 pixel CSA output from CMOS matrix => SMA cable => osc. scope
- ~10 Digitial signal output from EOC
- 6 DLL output
- LVDS Transceiver test between EOC and DAQ
  - Tx and Rx driver study
  - digital circuits for data serializer

Comments from Ivan on Draft v0.4.1

Daniela's comment:

I read the tracker section and found that the structure of the reference TDR has improved.

Nonetheless, the Barcelona version still needs substantial editing. In addition, some figure captions — for example, Figure 4.8: "For we could not completely handle high-lumi Z mode now, as well as the major difference between high-lumi Z with Z mode is luminosity which means their hit rate distribution is similar, the hit rate distribution of high-lumi Z would not be shown here." — indicate that there is still an unresolved issue with the high-lumi Z mode.

This should be addressed carefully.

Outer Tracker(OTK)

Findings

- The Outer Tracker (OTK) of the CEPC is a large area tracking system designed to provide precision timing and position measurements, complementing the inner tracking systems and the central Time Projection Chamber (TPC). It plays a critical role in improving momentum resolution for high-momentum tracks and mitigating performance degradation of the TPC in high-luminosity operations, where ion backflow-induced space charge can distort the drift field and impair tracking accuracy. The OTK is based on AC-coupled Low-Gain Avalanche Detectors (AC-LGADs) arranged as microstrip sensors, capable of delivering ~10 μm spatial and ~50 ps timing resolution, covering approximately 85 m^2 across the barrel and endcap sections.
- Since the October 2024 IDRC review, the CEPC OTK system has made significant progress in response to the committee's recommendations. The AC-LGAD sensor design was updated, reducing the baseline size from approximately 8 × 5 cm^2 to 4 × 5 cm^2 to improve timing performance and manage higher particle rates. A new prototype sensor layout was submitted for tape-out in February 2025, featuring a variety of strip lengths, pitches, and electrode widths to optimize capacitance, noise, and spatial resolution. In parallel, the LATRIC readout ASIC was finalized and submitted for tape-out in April 2025, integrating all main functionalities. Mechanical and thermal simulations were also updated, confirming stable operation under a heat flux of 300 mW/cm^2.

Comments

- The latest submission of the redesigned AC-LGAD sensor marks a key step toward determining the optimal strip geometry and layout for the OTK system. By systematically varying strip length, p-well doping, electrode width, pitch, and implementing isolation structures (e.g., trenches) to reduce capacitance, this prototype will provide crucial data to balance timing resolution, position resolution, power dissipation, and occupancy, ensuring the final design meets the stringent performance and rate requirements of the CEPC detector.
- The LATRIC ASIC is a critical demonstrator, consolidating all essential functionalities required in the OTK readout chain into a single chip. It includes a low-jitter analog frontend, clock generation via PLL, coarse-fine TDCs, internal calibration circuits, and a data readout architecture with serializer and control interfaces. Its successful validation will be essential to confirm the feasibility of a compact, low-power, fully integrated readout solution for the AC-LGAD-based OTK system

Recommendations

- To fully exploit the potential of this design iteration, it is strongly recommended to conduct exhaustive performance characterization of the newly submitted AC-LGAD sensors in test beams. These studies are critical to experimentally validate the effects of strip length, pitch, electrode width, n^+-well doping, and isolation structures on timing and position resolution, power dissipation, and occupancy. Given the importance of timely feedback 9 and the current unavailability of the LATRIC ASIC, it is advised to perform these measurements using fast discrete amplifiers until the LATRIC ASIC becomes available.

Following the submission of the new AC-LGAD prototype in March 2025, we are actively preparing the test setup for comprehensive sensor characterization. Once the sensors are received from tape-out, we will perform a series of measurements using radioactive sources and laser systems. To fully evaluate sensor performance, our dedicated team has a plan to carry out thorough assessments, including test beam studies.

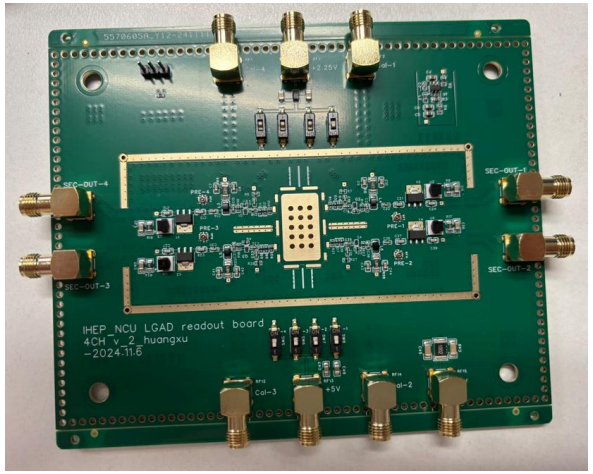

- 4-channels readout boards has been fabricated for AC-LGAD testing
- 2-stage amplifiers, Gain~70
- Signal shape has significantly improved, showing no oscillations.

Recommendations

OTK

- The collaboration should continue evaluating other LGAD sensor options and should closely follow novel developments, particularly the trench-isolated DC-LGADs currently under investigation by the team.

We are open to exploring various LGAD sensor options to achieve high performance through the optimization of spatial resolution, timing resolution, and power efficiency. Trench-isolated LGADs are particularly important, as the isolation structure reduces sensor capacitance and thus lowers power consumption. In addition to the LGAD prototype submitted in March, as previously reported, we are currently preparing another tape-out that includes trench-isolated designs with both DC- and AC-coupled variants. We will continue to closely follow ongoing developments and conduct detailed evaluations to identify the most suitable sensor technology for our application.

Recommendations

- It is recommended to ensure that the LATRIC ASIC is made available for sensor bonding as early as possible to enable realistic and fully representative characterization of the AC-LGAD sensor performance. Integrating the final readout ASIC with the sensor is crucial to obtaining accurate estimates of timing, position resolution, and power consumption. Given the critical role of the OTK in correcting space charge distortions in the TPC, it is essential that the OTK be robustly designed with service granularity in mind, exploring all known failure modes and developing strategies to mitigate them.

We are fully aware of the critical importance of the LATRIC ASIC, as it is essential to the success of the OTK. Our ASIC team, which includes several senior designers, has made substantial efforts to ensure the reliable and timely delivery of functional chips. The development process is carefully planned and regularly reviewed, with ongoing technical discussions to track progress and resolve challenges. All efforts are focused on accelerating the design and verification phases, so that the ASIC can be made available in a timely manner for sensor bonding and realistic performance characterization.

Comments from Ivan on Draft v0.4

- Concerning the chapter organization, this is significantly improved, facilitating the reading. The ITK and OTK dedicated sections now share the same subsection structure (design,electronics, mechanics, sensor technology and ASIC, and future plans); they also cover the important aspects of alignment, background estimations, and performance. As mentioned, the removal of the alternative sensor technologies for ITK and OTK has greatly improved the draft's readability.

We thank the Referee for the comments. Your suggestions have greatly improved the clarity and organization of our paper. We appreciate your positive feedback on the chapter structure and the revisions implemented.

Comments from Ivan on Draft v0.4

- The remaining content is very similar to the previous version; I noticed that the background hit rates are now lower than those presented in April's version, and the major missing part remains the definition of an approach to tackle the TPC performance degradation due to ion back-flow, but this will likely require considerably more time to address.

We are actively studying and improving the shielding design to reduce beam induced background. Since the last review, we have updated the MDI shielding design, which has enabled us to achieve a further reduction in background levels.

Comments from Ivan on Draft v0.4

- Anyhow, we may recommend including a subsection in the chapter mentioning the TPC response degradation issue, along with an overall strategy to mitigate it. This addition would send the message to the reader that they are aware of the importance of the issue and are actively working on how to resolve it. This section could be also fit in the TPC chapter, though.

TPC

Findings

- The Time Projection Chamber (TPC) with pixelated micro-pattern gaseous detector readout has been chosen as the baseline for the central tracker. It offers continuous 3D tracking with minimal material budget over a large volume and provides particle identification (PID) capabilities. This is a solid and well-justified choice for the Reference TDR, building on extensive past TPC experience at lepton colliders and more recent developments from ALICE, the LCTPC, and DRD1 collaborations. Several technological advances have recently been achieved; notably, a novel ultra-light QM55 carbon fiber material is now used to construct the TPC cylinder.
- However, realizing the TPC as the tracker will require further significant efforts, particularly in mechanical design, structural integrity, and achieving uniform magnetic field conditions (see also the comments and recommendations in the Magnet chapter). Full simulation and digitization tools, based on the software framework and reconstruction algorithms, have been developed and must now be used to produce an updated set of performance plots (e.g., separation power plots).
- The possibility of using a drift chamber as an alternative tracking option is also presented in the TDR.

Comments

- Since the IDRC 2024 review, significant progress has been made in the simulation of spacecharge distortions. For CEPC Higgs and low-luminosity Z runs, the maximum distortions after 3 meters of drift were found to be approximately 10 μm and 150 μm, respectively. Nevertheless, these figures require further verification, and careful evaluation of beam-related background effects must continue. In the longer term, dedicated simulation efforts are needed to develop and refine a "datadriven" approach for extracting space-charge corrections, based on the alignment and correction models developed for the ALICE TPC

- The TPC has been selected as the baseline main track detector in the CEPC TDR. The simulations and analysis of beam-induced background in the TPC have been continued with some collaboration (KEK, DESY). The low-energy photons (MeV) are the main source of positive ions in the TPC, both in the Higgs and low luminosity Z modes. The space charge density in the CEPC TPC is only about 1/60 of the ALICE TPC in the Higgs mode if the ion-backflow (IBF) can be suppressed to the primary ion level. Some optimization strategies are proposed to further reduce the backgrounds.
  - Reducing the beam lost rate.
  - Adding shielding after the lumiCal.
  - Developing a dedicated distortion correction algorith

Comments

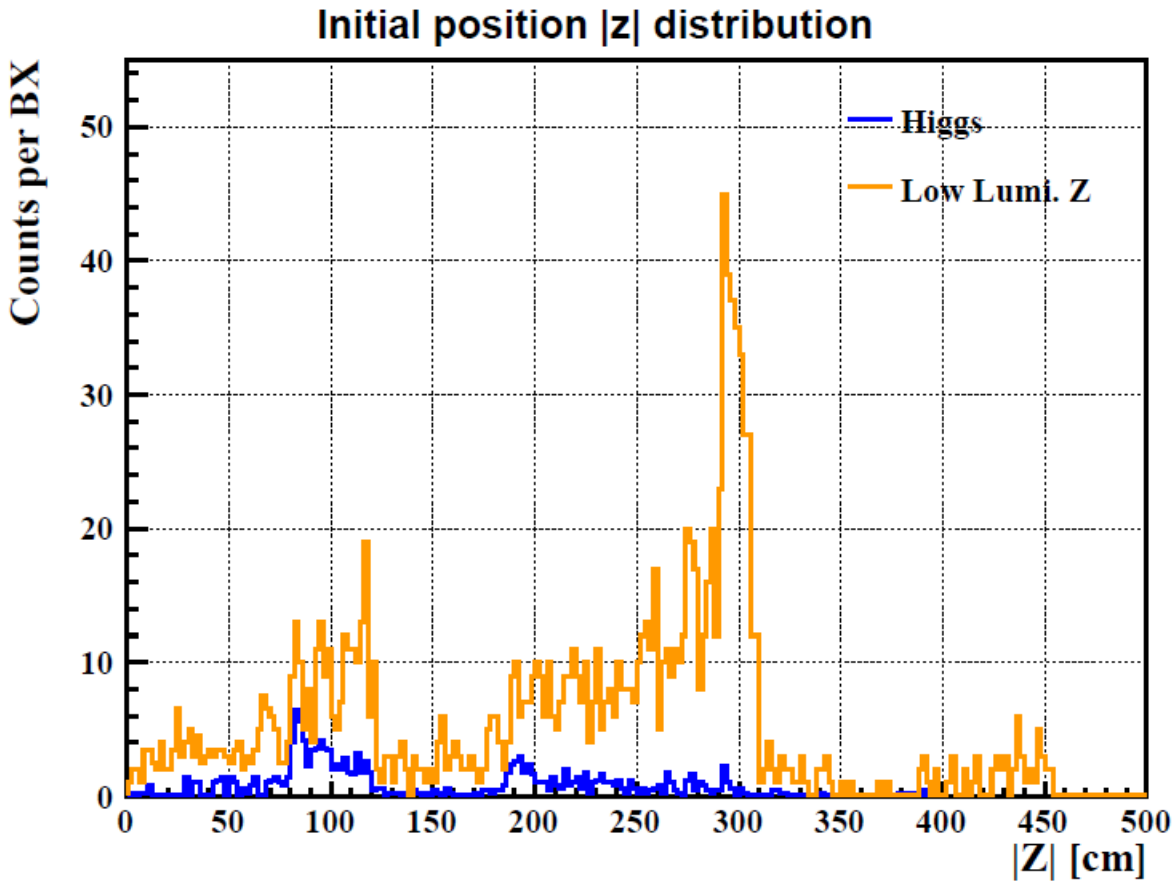

The initial position |z| distributions of photons interacting with the T2K gas in two running modes.

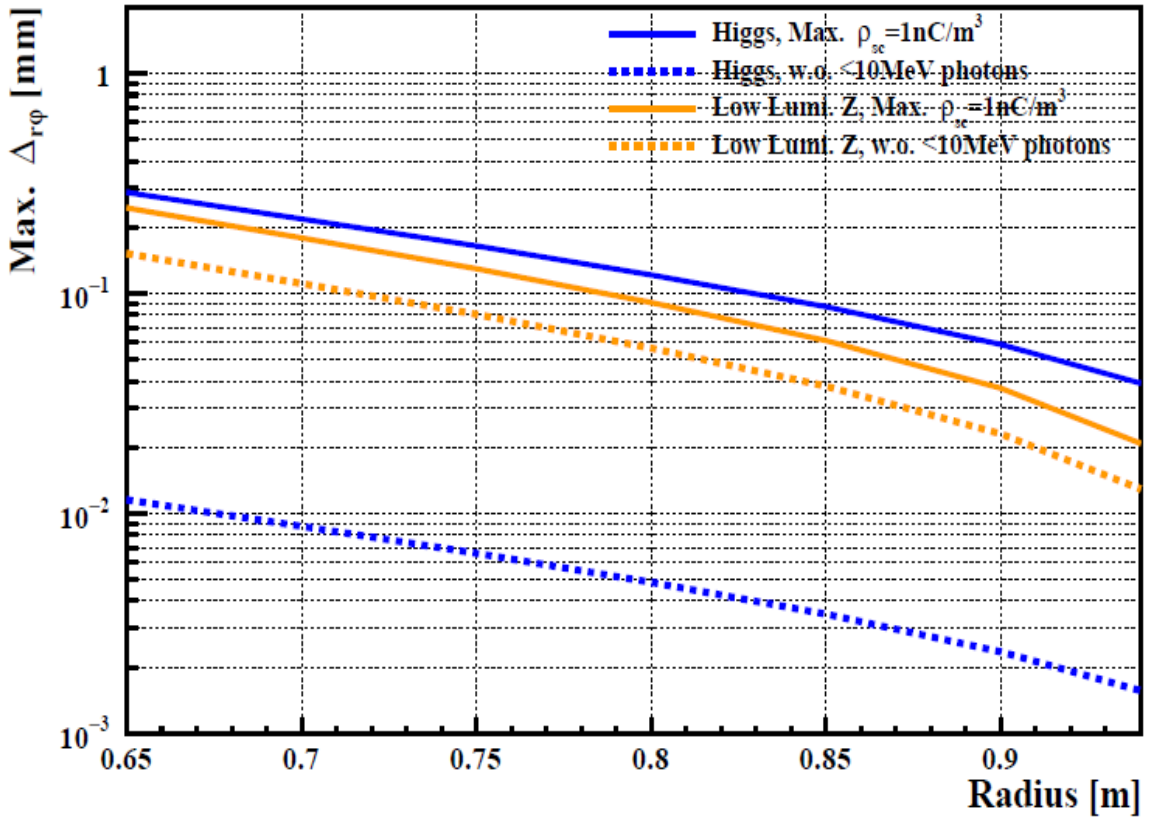

The maximum Δrφ after 2.75 m drift length as a function of radius.

Comments

- The choice of the pixel readout chip (TEPIX) with a 500 × 500 μm² pixel size is currently driven by power consumption considerations. A TPC module prototype with 10 × 300 readout channels (using 24 TEPIX chips) has been developed and is planned for beam testing at DESY in 2025. Larger prototypes will need to be developed and tested during the EDR phase. Optimization of pad size and gas mixture must be finalized, clearly distinguishing between the digital pixel readout case and the pad readout case. These two approaches lead to distinctly different electronics requirements, particularly regarding the need for analog-todigital conversion in the pad case.

- Within the framework of the LCTPC and CERN DRD1 international collaboration, our research group has booked a beam test at the DESY Institute in Hamburg, Germany, scheduled for November 2025. We will use a 5 GeV electron beam to test the performance of a TPC prototype, providing solid experimental evidence for the existing pixelated readout, The functions of the analog-to digital conversion and digital readout mode have been started to do R&D in our collaboration group. The full size prototype will be considered aslo.

- If the alternative drift chamber option is pursued, it will be necessary to identify a hydrocarbonfree gas mixture that maintains the required performance characteristics

- Thank you for the suggestion. We will focus on the TDR document and the baseline design detector in the near future. Some updated simulations and optimizations of the gas mixture will be carried out beyond the TDR of CEPC.

Comments

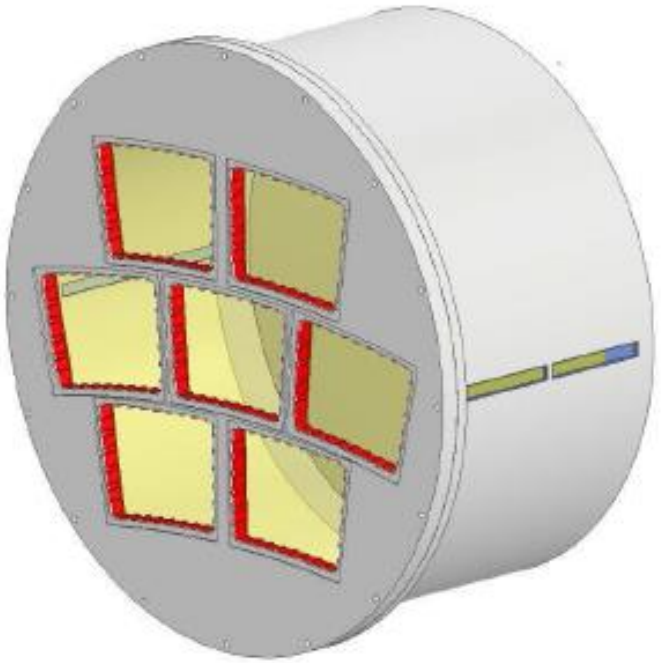

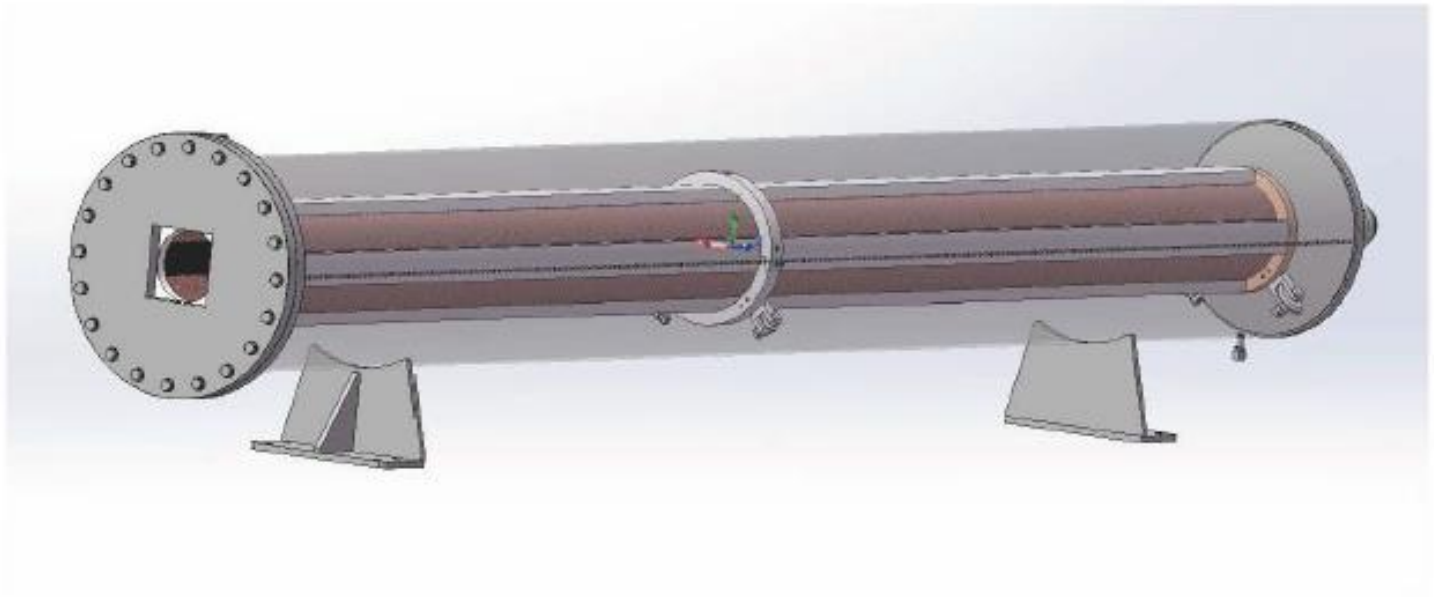

Study of the TPC prototype assembled with seven modules using UV laser and cosmic rays, the module size is same as the TPC module in TDR (Left). The prototype of the 2.9m full-length TPC is primarily designed to study the electric field and the electron drift (Right).

Recommendations

TPC

- The structure of the TDR chapter needs better definition and further consolidation; some figures presented during the review must be updated in the document.
- The structure and content of Chapter 06 have been updated following discussions within the CEPC community.. The new version of the document will be prepared.
- Ion backflow during operation in low-luminosity Z-mode remains the primary concern. Further simulations of TPC space-charge distortions induced by beam-related backgrounds are necessary to optimize the Machine-Detector Interface (MDI). New module prototypes implementing advanced ion suppression techniques (e.g., double-grid structures or graphene layer coatings) should be studied.
- After detailed discussions with Prof. Imad, we have explored the potential of graphene technology to control positive ion feedback. This exploration involved researching graphene membrane conversion technology and engaging with various institutions. Specifically, we have initiated collaborative research efforts with Shandong University, CEA-Saclay, Lyon University, the University of Bern, and CERN. These collaborations aim to leverage the unique properties of graphene to mitigate positive ion feedback, thereby enhancing the performance and reliability of our detectors.

Finding on Draft v0.4.1

- The Barcelona version of the TPC chapter shows clear progress in terms of section organization and clarity compared to the previous drafts:
  - The overall structure is improved, with more logical sub-sections and better-defined description flow;
  - The mechanical design aspects (inner/outer cylinders and support structures) are more consistently described;
  - There is a better introductory explanation of the role of the TPC as the central tracking detector and its importance for the PID performance;
  - Prototype development efforts are more explicitly referenced, including pad readout, based on micro-pattern gas detector studies;
- These editorial and content enhancements are really appreciated and help to bring the chapter into more advanced stage. However, several technical issues raised in the previous review remain (partially) unresolved or are addressed only qualitatively.

Comments on Draft v0.4.1

1. Space-Charge Distortion and Ion Backflow

- The chapter still lacks a quantitative description of space-charge distortion and its impact on tracking;
- Mitigation strategies (e.g., double GEMs, gating grids, graphene coating) are mentioned, but not developed or prioritized for future studies;
- There is no indication or explanation of how correction strategies (e.g., ALICE-like data-driven approaches) can be implemented, at least qualitatively;

Comments on Draft v0.4.1

2. Tracking Performance and Simulation

- There is no significant update on spatial or momentum resolution, dE/dx performance, tracking efficiency, or fake rate studies;
- Performance plots, especially in conjunction with the ITK/VTX system, are missing or remain in a preliminary stage;

Comments on Draft v0.4.1

3. Pad Size and Readout Architecture

- We understand that the choice between pad and digital pixel readout can not be finalized at this stage and remains uncertain. Still, some comments about the implications in terms of electronics complexity, data volume, and reconstruction performance would be beneficial;
- The absence of a baseline readout definition introduces uncertainty in downstream systems (DAQ, reconstruction).

4. Gas Mixture and Ion Backflow Suppression

- No clear indication about choice of gas mixture is presented. Therefore, the interplay between gas properties, backflow suppression, and long-term stability cannot be sufficiently discussed.

Recommendations on Draft v0.4.1

Acknowledging that the time for substantial new studies is limited, we recommend the following clarifications to the TDR text, to the extent they are feasible at this stage:

- 1. Acknowledge open issues: clearly define which aspects of the TPC design (e.g., ion backflow mitigation, space-charge correction, gas mixture optimization) are still under investigation, and describe the R&D or simulation path that will be followed to finalize these aspects at the next stage;
- 2. Clarify target performance: For each open topic (e.g., ion backflow, pad size), provide the expected performance goals (e.g., maximum tolerable distortion, acceptable ion backflow level, target spatial resolution) that guide the ongoing design effort;
- 3. Readout architecture: While a final decision may not be ready, describe the criteria that will drive the selection of the readout scheme and how each option will be validated. Summarize the impact of this choice on reconstruction, electronics design, and system integration. Clarify what is called a pixel TPC (digital readout) and a pad TPC with ADCs. Quantify power consumption in the two cases and document cluster counting for a digital readout;
- 4. Simulation plans: Summarize how future simulations will validate TPC performance in full physics conditions (e.g., displaced vertices, Z-mode operation), if feasible;

Editorial additions

- Include a concise summary table linking current detector parameters and technologies to physics requirements. This will help contextualize the design and highlight where validation is still pending;
- Streamline English and revise references;

ELECTROMAGNETIC CALORIMETER

Findings

- The high-granularity crystal ECAL is a recently proposed concept designed to be compatible with particle flow algorithm (PFA) reconstruction of jet energy within a homogeneous structure. The calorimeter is modular, with the fundamental detection units consisting of long orthogonal BGO crystal bars, read out at both ends by SiPMs.
- Achieving high granularity at an affordable cost requires making strategic choices and compromises, guided by specific performance benchmarks. The **team has made steady progress** in understanding the performance and optimizing the performance-cost balance, using the ECAL standalone energy resolution and PFA jet resolution as primary benchmarks.
- The baseline granularity was recently updated to 15×15×40 cm^3, resulting in a significant reduction in the number of readout channels and associated power needs. Simulations indicate that, even with this updated configuration, the calorimeter meets the target requirements for boson-mass resolution and standalone electromagnetic energy resolution. The **overall performance remains excellent**, despite some degradation in π^0/γ identification and two-photon separation; the latter may potentially be recovered through improvements in offline reconstruction methods.
- A **full-scale prototype** with the updated granularity is planned. Current simulation studies and experimental results from similar granularities provide confidence that the ECAL performance and component requirements are sufficiently understood, despite limitations in previous test beams due to electron beam spread. The team is also aware of the need for further progress beyond the reference TDR, particularly in **defining QA/QC aspects** for the components.

Comments (1)

- The ECAL standalone energy reconstruction requires an energy threshold of 0.1 MIPs (as shown in Fig. 7.17), whereas the PFA jet reconstruction, based on fast simulation, adopts a higher threshold (Fig. 8.2). The ECAL team acknowledges the need to further develop and refine particle flow algorithms, photon identification at low energies, and π^0/γ separation to fully exploit the calorimeter's potential.
- The timing specification of 0.5 ns for MIPs was not strongly motivated. This corresponds approximately to the time spread across a full bar and is insufficient to provide significant benefits for event reconstruction. Additionally, the current time resolution analysis appears suboptimal. The team acknowledges that a deeper understanding of timing response and its potential use is needed, although this is not a priority at this stage.
- Crystal transparency variations are significant. While progress has been made toward developing a calibration plan using collision events, a quantitative demonstration that the precision and event rates are sufficient for monitoring response evolution across the detector is still missing.
- The non-linearity of the SiPMs poses a potential risk to the constant term in the energy resolution. Although compact photon detectors with more linear responses (such as APDs) were noted, SiPMs are preferred for cost and design uniformity reasons. However, SiPMs will require per-channel calibration, and possibly sorting during construction, along with continuous in-situ monitoring and corrections.

Comments (2)

- Prototyping with close-to-final components is essential to confirm performance. Using existing readout ASICs can help decouple detector characterization from electronics debugging and allow parallel progress rather than sequential steps.

- The committee was pleased to see a substantial effort in understanding the impact of gaps between modules. However, the mechanical design and service layout within the gaps remains sketchy, and some components, such as the cooling plates, could be prone to underperformance.

- From a stylistic perspective, the TDR would benefit from an upfront presentation of the key performance benchmarks and detector specifications, followed by a focused discussion of the performance-cost optimization supported by R&D and simulation evidence. The detailed discussion of alternative options currently in Section 7.2 could be summarized briefly and moved to an appendix.

Recommendations

- Continue developing a **full-scale prototype** with the final geometry (using existing readout ASICs) and aim to confirm performance in an electron beam with low momentum spread.
- Further **refine calibration strategies** to ensure that necessary stability in transparency, linearity, and uniformity can be achieved in situ, without relying on a dedicated monitoring system.
- Advance preliminary engineering of the gaps between modules and fully assess their impact on reconstruction performance.

Comments on Draft v0.4.1

- General comment:
- There is no mention of separation of showers or individual particle depositions. The parameters mentioned are energy resolutions without mentioning the segmentation (granularity) needed to achieve particle flow performance. We suggest adding mention of needed segmentation or granularity.
- Line by line comments:
- line 1475, 1481: - reference to just LEP for last gen e+e-. Suggest "LEP and SLD at SLC"
- line 1490: "the key ingredient" I suggest "a key ingredient"
- lines 1493-1494: We suggest expanding the sentence to "We propose to use BGO crystals as full absorption ECAL which will significantly improve energy resolution, which is essential for optimal H-> gamma gamma detection, for example."
- line 1496: "18 longitudinal layers providing 24 radiation lengths" → "providing 24 or more radiation lengths", since there are more than 24 radiation lengths. for much of the barrel
- line 1499: "fully contain electromagnetic showers." → "maximize containment of electromagnetic showers.", because, strictly speaking, there is still some leakage.
- line 1524: "typical" would be better as "the typical" and "result" should be plural "results".

Comments on Draft v0.4.1

- The EM calorimeter chapter has been substantially restructured. It now presents directly the design choice and comments on alternatives at the end of the chapter. This addresses one of the comments that were raised in the April review and benefits the clarity of the information flow. The text has been polished and shortened in several parts, improving readability. However, the large restructuring poses a challenge to the review process, as we are largely facing a new document.
- The overall design and specifications are essentially the same, except a few notable changes, which require further considerations:
- The MIP requirement for the MIP light output has been raised from 200 to 300 p.e./MIP. While this makes the 0.1 MIP threshold for signal-to-noise ratio easier to achieve, it makes the requirement for the linearity up to 3000 MIPs (set by the maximum energy deposition from e showers for the CEPC operated at 360 GeV) more difficult to be met. Additionally, tests with prototypes show that the light yield of bars in the baseline bar configuration (1.5x1.5 x 40 cm3) are 400 pe/MIP (L.6527), thereby requiring linearity up to 106 pe and beyond. Simulation studies show that the linearity requirements are met (Section 7.3.5). However, these studies assume the nominal 300 pe/MIP and not the measured output of 400 pe/MIP for the baseline design choice for the BGO bars. Additionally, the study is limited to photons from the H → γγ decay for operation at 240 GeV, which have an energy deposition up to about 1500 MIPs (Fig. 7.5b). The SiPM dynamic range is further discussed in Section 7.4.2.2, with numbers that appear inconsistent with other parts of the TDR. For example, it is stated (L.6586) that a maximum deposition per bar of 45 GeV corresponds to 5x105 pe. However, at L.5984 it is stated that the MPV for a MIP is 13.3 MeV, which converts into 3383 MIPs for a 45 GeV energy deposition. At 300 pe/MIP, this gives already 106 pe. At 400 pe/MIP this is above 1.3x106. In summary, the effect of non linearity over the full range and up to 106 p.e. (or beyond) with SiPMs having 250k pixels does not appear to be sufficiently documented.
- The specification about radiation hardness requirements has been dropped from the list (Table 7.1). A statement on the response stability of the BGO vs the ionization dose is needed in the section where the crystal choice is discussed, even if this is not translated into a specification.

Comments on Draft v0.4.1

- There are a few inconsistencies in the requirements about energy resolution. At line 5932 it is "$\sigma E/E$ ≤ 2%/root(E)" while at L.1501 it is required an "energy resolution of <3%/root(E)". In other places the energy resolution is required to be less than 3% (Table 7.1) without specifying any energy dependency. Then there are instances where both the stochastic and the constant term are indicated (L. 6851 and L.1321, again with some inconsistency between 2% and 3%). Please clarify and distinguish clearly between the requirement and what is achieved. For example at L.6851, if the requirement is 3% and you achieve <2%, you can simply state that the requirement of <=3% is achieved.

Comments on Draft v0.4.1

- The discussion about timing performance (Section 7.4.3) remains confusing. The time resolution is defined as “the standard deviation of the time difference of the time stamps of SiPM signals from the two ends of a crystal”. This quantity is not independent of the hit position and does not correctly quantify the precision with which the position of a deposition can be reconstructed. A deposition in the centre of the bar, would give a $\Delta t = 0$ with an RMS from the resolution of the device. A deposition near the ends of the bar would give a distribution with the same RMS centered at $\Delta t = +/- L/2v$, where L is the bar length and v the velocity of the light in the crystal. For a uniform hit distribution, the RMS will therefore get a contribution from the propagation path of $L/(v \sqrt{12}) \sim 0.6$ ns for L=40 cm, v = 1.5c. This should be added in quadrature to the genuine time resolution from the detector and readout. In Fig. 7.31 at L=40 cm, the resolution is 0.7 ns, which is consistent with 0.6 ns from propagation (+) 0.4 ns intrinsic to the detector, which you can read from the measurement with L=2 cm crystals. At L=60 cm, your measured resolution is almost 1 ns, which is again consistent with an $L/(v \sqrt{12}) \sim 0.9$ ns (+) 0.4 ns. So, while your data show the expected behaviour, your interpretation of the results is different. At L 6602, you conclude that at L=40 cm, the resolution is 700 ps (500 ps per end), while your data indicate a resolution is 400 ps/MIP (280 ps per end), which would scale to a resolution of 100 ps already at 200 MeV (per crystal). A better measure of the time resolution is provided by the RMS of the sum of the two timestamps, because the sum of the two propagation times is independent of the hit position. A plot of this quantity should clarify what is the actual resolution. You may still have some dependence on the bar length, because the light output is lower for longer bars.

Comments on Draft v0.4.1

- Line by line comments (not exhaustive):
- -line 5914 - "It also detects neutral pions $\pi 0$ ...." → "It detects neutral pions $\pi 0$ ...." The current formulation (with “also”) is a bit strange to me since it actually detects the gammas from neutral pions and those were already mentioned in the previous lines.
- -line 5920 - "Moliere Radius" → "Moliere radius"
- -line 5935 - "at two ends." slightly better would be "at both ends."
- -line 5939+ and Fig 7.1: "contains over 400 long crystal bars”. It would be helpful here to re-state number of crystals in depth (18 specified much earlier on line 1496)
- -line 5963 - "ers.`necessitating" looks like a typo ".`" should be ", "
- -Figure 7.1: Here the "module" is shown as a "supercell". This is the first use of the term "supercell". Supercell is later referred to in section 12, but not until then. A clarification of these two different references should be added.
- -Table 7.1 "EM energy resolution < 3%". Shouldn't this be energy dependent? Perhaps, add <3% above xx GeV.
- -lines 6009 - 6010: "A typical 40 × 40 cm2 module employs 1.5 × 1.5 × 40 cm3 crystal bars". It would be helpful here to state there are 18 layers.
- -lines 6861-6863: "~ 285,000 crystals" "571,000 SiPMs". As there are two SiPMs per crystal by design, make the two figures a factor two: either ~285,000 and ~570,000 or 285,500 and 571,000.
- -line 6851 "to achieve an EM energy resolution of $\sigma E/E$ ≤2%/root(GeV) ⊕1%" should be root(E(GeV)). Please correct also the requirement on line 1321 "$\sigma E/E$ ≤ 3%/ root(E(GeV)) ⊕ 1%," (and make them consistent)
- -lines 11299-11301: "The ECAL supercells, mentioned in Section 7.2, are used for the preliminary trigger studies.". We don’t find mention of supercells in section 7.2, where discussion of ECAL elements are modules. If the ECAL supercells are identical to "modules" the terminology used in Section 7, it would be helpful to state that here.

Feedback to IDRC Recommendations (1)

- Continue developing a **full-scale prototype** with the final geometry (using existing readout ASICs) and aim to confirm performance in an electron beam with low momentum spread.
  - Developing a full-scale technological prototype is planned for next 3-4 years, by integrating crystal bars, readout boards embedded with SiPMs and ASICs, a cooling system within a light-weighted mechanical structure
  - Electron beam with low momentum spread: this would require quite significant efforts to control.
    - Crystal ECAL prototype shows EM resolution better than 2%, which requires beam spread well below 1%.
    - (e.g. DESY 1-6 GeV electron beams: momentum spread on the order of 10% at 1 GeV)
  - Test beam facilities are listed:
    - CERN PS-T09 is the primary option (with our best understandings and hands-on experiences). But due to the coming Long-Shutdown (LS3) during 2026-2028, we will also need to consider alternative options.
    - Light sources in China: need to investigate synchrotron radiation light sources (e.g. BSRF, HEPS)
    - KEK 1-6 GeV electrons: need to understand lowest possible momentum spread → trade-off between rate and spread.

Feedback to IDRC Recommendations (2)

- Further **refine calibration strategies** to ensure that necessary stability in transparency, linearity, and uniformity can be achieved in situ, without relying on a dedicated monitoring system.
  - Crystal transparency: ECAL simulation with TID mapping in 3D and finer granularity in time domain BIB doses (CEPC Bhabha production rate, statistics requirement for the target calibration precision and transparency degrade rate)
  - Systematic studies and descriptions on factors with significant impacts to the ECAL performance
    - Crystal: (1) response uniformity along the bar length, (2) batch uniformity in mass production and quality control
    - SiPM: (1) response linearity, (2) batch uniformity in mass production
    - ASIC: (1) ADC linearity, (2) switch between different gain modes, (3) batch uniformity in mass production
    - BIB: (1) extra hits mixed in signals (time window), (2) crystal transparency degrade after calibration, (3) SiPM degrade due to NIEL
    - Temperature: (1) gradient (monitoring data for corrections), (2) fluctuation (stability)
    - Geometry effects: (1) gaps between crystals and modules, (2) insensitive materials, (3) longitudinal shower leakage
  - SiPM non-linearity calibration scheme (details in next page)

Feedback to IDRC Recommendations (2)

- Detailed calibration scheme on SiPM non-linearity effects
- Considerations
  - SiPM non-linearity effects are studied by including SiPM pixel recovery during the relatively long BGO scintillation time (typ. 300 ns), which further increases the effective number of SiPM pixels
  - Calibration is first done in an off-detector way, by extracting key parameters related to the SiPM non-linearity effects via the SiPM QA/QC database (e.g. breakdown voltage, PDE, interpixel crosstalk, etc.)
  - Apply these parameters to all SiPMs in ECAL after detector assembly and use them for commissioning
  - During operation, use Bhabha events as an abundant in-situ calibration source to monitor and calibrate SiPM non-linearity
- Plans beyond Ref-TDR scope
  - To validate the SiPM non-linearity simulation model via laser and beam tests
  - To test batches of SiPMs for non-linearity calibrations: to extract QA/QC parameters and to validate the proposal above

Chapter 7: IDRC recommendations and comments

- Advance preliminary engineering of the gaps between modules and fully assess their impact on reconstruction performance.
- Current status
  - ECAL electronics and mechanics engineers work together on the engineering designs, including readout boards, cooling sheets and active cooling pipes
  - An energy-correction algorithm has been developed to correct and recover the energy loss due to the showers in the module cracks
  - Plots of EM performance have been updated by including incident photons uniformly distributed around an ECAL module including crack regions
- Plans
  - To address the engineering challenge of the long-term reliability of cooling pipes and valves and precautions to leakage risks
  - ECAL mechanics engineer will investigate possible measures: e.g. “seamless” pipes, humidity monitoring, valves in case of leakage

Chapter 7: IDRC recommendations and comments

- Single photon reconstruction performance
  - IDRC review: need to describe in a more clear and consistent way how to reconstruct photons
- Current status
  - Two different algorithms to reconstruct photons in the low energy region (new) and high energy region (CyberPFA)
  - A new plot of single photon reconstruction is updated in the TDR

Chapter 7: IDRC recommendations and comments

- Detailed calibration schemes on crystals and SiPMs (BIB irradiations)
  - Requires “finer granularity” in time periods for estimation of radiation doses
- Current status
  - BIB radiation doses are estimated for each year
  - BIB simulation samples provided with 20,000 bunching crossings, then multiplied by a scaling factor (e.g. 7,000 hours per year for CEPC operation)
- Plan
  - To update BIB radiation doses using different scaling factors (e.g. per week/month)
  - To determine how frequently crystal-SiPM calibrations should be performed
    - Aim: “dynamic” changes in crystal light output are reflected in Bhabha events
    - Balance of data statistics and crystal-SiPM degrade speed
    - Bhabha event rate per module can be applied for data statistics estimation

Chapter 7: IDRC recommendations and comments

- ECAL timing performance
  - IDRC comment: lack of justifications or motivations for the timing resolution specified (0.5 ns per end)
- Plan
  - To investigate potentials of ECAL timing in mitigation of Beam-Induced Background effects, especially excessively high hit rates in certain regions (e.g. barrel ECAL inner layers, endcap modules close to the beam pipe)
- Ongoing studies
  - This timing study would be complementary to the BIB mitigation scheme by increasing energy thresholds for certain ECAL layers (0.1 MIP → 0.2 or 0.3 MIP)
    - Balance between EM performance and BIB hit rates

HADRONIC CALORIMETER

Findings

- A key innovative feature of the Hadronic Calorimeter (HCAL) is the large sampling fraction achieved through the use of heavy scintillating glasses (GS). The proposed layout offers the potential to significantly improve the PFA resolution by enhancing the stochastic term of the single-particle energy resolution. The committee acknowledges that the team is highly motivated and is making steady progress toward this ambitious design.

Findings

- The proposal is reasonable but aggressive. Detector specifications and performance benchmarks are clearly defined; however, considerable work is needed to bring the GS-HCAL baseline choice from its current R&D phase to a full-scale detector.

- --The primary objective of this section is to validate that the GS-HCAL design meets the CEPC physics program's core performance criteria, including hadronic energy resolution, linear response across the energy spectrum, and mitigation of beam-induced background effects on signal reconstruction. Leveraging extensive simulation studies in the absence of prototype data, we demonstrate the design's compliance with these requirements. In the new version in **Section 8.5 (** simulation and performance).

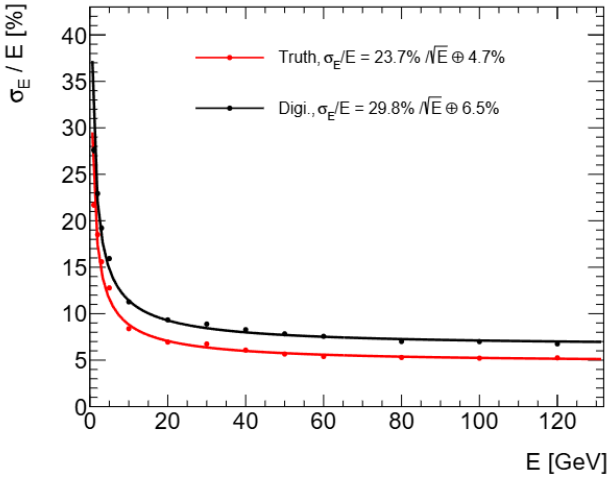

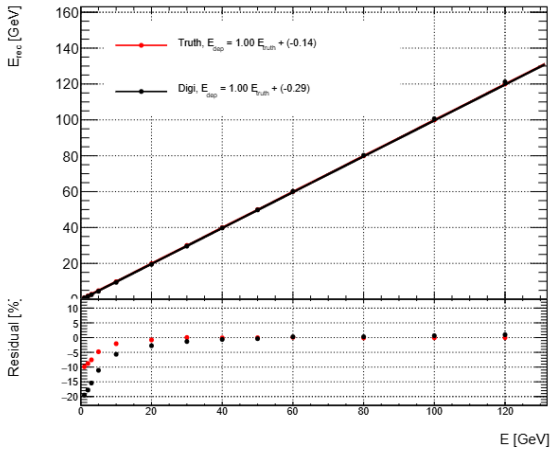

The estimated energy resolution of $\sigma E\ /E$ = 29.8%/$\sqrt{E}$ $\oplus$ 6.5% and an energy linearity within 2% before calibration, outperforms the stochastic term of traditional HCALs.

Findings

- For instance, during the review, the team was uncertain about the origin of the constant term observed in the hadronic energy resolution, a result obtained from idealized simulations with only limited hardware effects included.

- --The relatively large constant term in the energy resolution is attributed to the longitudinal leakage in this 6 λ_I design, which is constrained by the total detector volume and cost. Specifically, for hadronic showers that initiate late or develop with great depth, the GS-HCAL configuration could permit a substantial portion of the energy to escape. To verify the hypothesis that longitudinal leakage was the cause of the observed discrepancy, we increased the depth of the GS-HCAL from 48 layers (6 λ_I) to 80 layers (10 λ_I). With 48 layers, the calorimeter generated a pronounced tail in the energy distribution at higher beam energies, leading to an extracted constant term of approximately 4.7%. However, when the calorimeter depth was extended to 80 layers, this tail decreased significantly, and the constant term dropped to around 2.9%. The significant improvement in the constant term upon increasing the depth of the GS-HCAL supported the hypothesis that shower leakage, rather than an intrinsic design flaw, was responsible for the inflated constant term. The deeper calorimeter configuration effectively contained the hadronic showers, demonstrating the performance characteristics of a well - functioning hadronic detector.

Findings

- The committee is pleased to note that the next step is the construction of a large-scale prototype.

- --Yes, in the new version of the HCAL-TDR, the new design of the prototype has already described, as in the **Section 8.4.8**. The construction and testing program proceeds in phases. A 3×3×7 mini-prototype is currently under construction for initial beam tests at CERN in October 2025. The full 8112-channel prototype is scheduled for completion by end-2026, with cosmic ray testsplanned at IHEP and subsequent beam tests preferably at CERN in 2027. This prototype implements a steel-scintillator sandwich structure in a compact 0.6 m^3 volume (52 cm × 52 cm × 130.6 cm). The primary objectives are to validate the novel GS technology at larger scale and collect hadronic shower data for shower profile studies and PFA optimization, which is unavailable from existing calorimeters. This prototype contains 8112 GS tiles arranged in 48 layers, serving as a critical testbed for the full GS-HCAL systems. Each scintillator layer consists of 169 tiles (13×13 array) with individual cell dimensions of $40mm \times 40mm \times 10mm$, optically coupled to 3 $mm \times 3\ mm$ SiPMs for readout. The steel absorber plates use S304 stainless steel (GB/T 4237-2015, equivalent to AISI 304) with 9.8 mm thickness. The system employs NDL-SiPM photodetectors with more than 30% photon detection efficiency and a gain greater than 10^5, selected based on their performance in previous experiments like GECAM and JUNO-TAO.

Findings

- In this prototype, each tile will be read out by four SiPMs, whereas in the final detector only one SiPM per tile is foreseen for cost reasons.

- --It is clear that there is only one SiPM for tile for the design and cost, as show in Figure 8.2, and detialed describe could be found in **section 8.2.1** (Single layer structure). In the **Section 8.4.5** (Measurements of GS with SiPM), it is shown the performance test result of the 4cm*4cm*1cm glass cell coupling with 1 piece of 3mm*3mm SiPM.

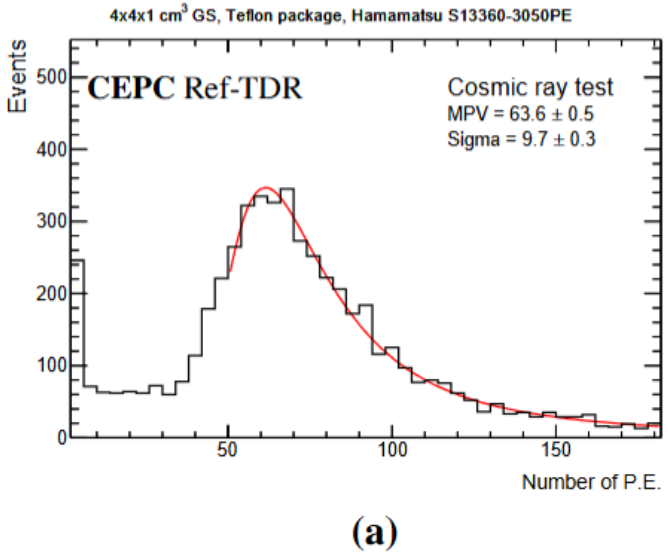

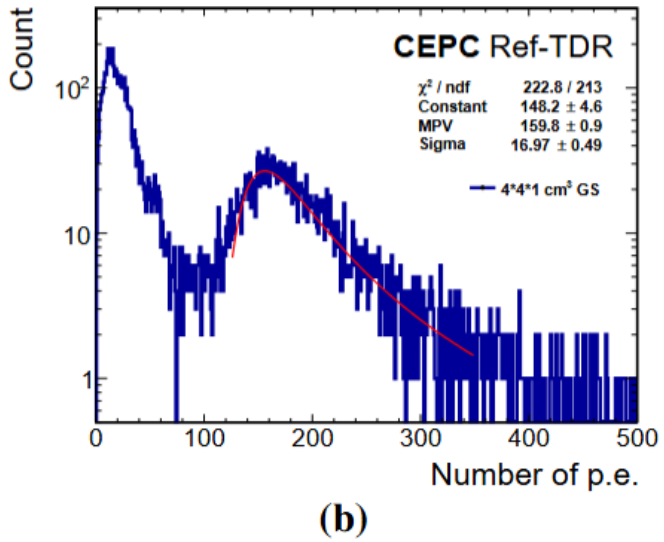

Cosmic ray test results of the GS tile measured using single SiPM.

(a) The measurement using Hamamatsu S13360-3050PE SiPM, resulting a light output of 64 p.e./MIP.

(b)The measured result is about 160 p.e./MIP using a Hamamatsu S13360-6025CS SiPM. The two results are consistent.

The difference is due to the different sizes of the SiPMs, and different PDEs.

Findings

- Regarding costs, the committee notes that the current cost estimate does not include the cost of PCBs, which experience shows can become a significant item for granular calorimeters due to the complexity of design and production.
- --the cost of PCBs has already included in the electronics part.

Findings

- It was also acknowledged that a sampling calorimeter based on plastic scintillator (PS-AHCAL), which is more mature and better understood, remains a viable fallback option. The committee encourages the team to continue pursuing the GS-HCAL option, while maintaining the PS-HCAL as a backup.

- --Yes, the GS-HCAL and PS-HCAL are both the options of the HCAL. the size of the GS or PS tile are the same as 4cm*4cm, has the same photon readout SiPM and the electrinics, the same size Box and Prototypes. If the GS R&D was falled, it will be easy go back to the PS-HCAL design. There is also a special **Section 8.6 (**Alternative HCAL options) introduce the R&D results of the RPC-SDHCAL and PS-HCAL.

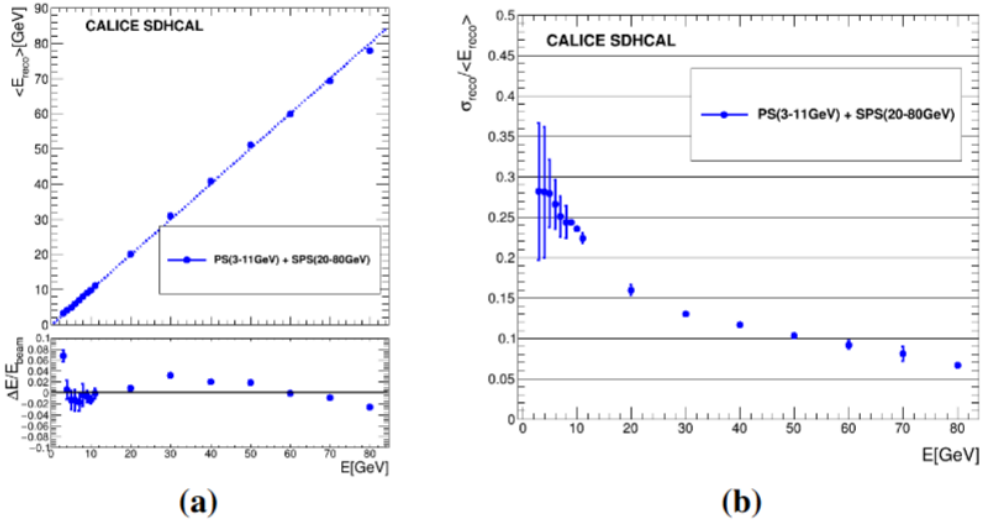

RPC-SDHCAL

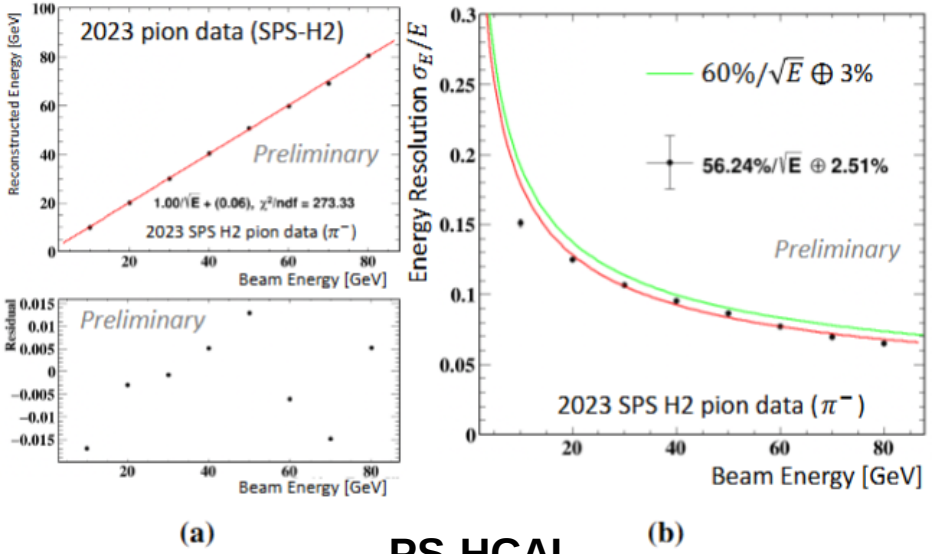

PS-HCAL

Comments

- Scintillating glasses represent new territory for hadronic calorimetry. The material properties, such as radiation length and hadronic interaction length, are not yet fully characterized. Although the decision to adopt this technology is well justified, it carries significant risk. Therefore, extensive prototyping and simulation studies are mandatory to validate the concept.

- --Yes, the study of the GS-HCAL option is only start in two years ago, and choise to be the baseline option on Aug.2024, there are lots studies need to do. After the IDRC review in Apr, the GS group has done lot research work for this new type of Glass Scintillator, and report the result in this new version of HCAL-Ref-TDR. In **Section 8.4.2** (Glass scintillator). In the old version of the TDR, there are two types of GS with the name as GFO and GFO+, new days we have make sure to use only the GFO Glass as the baseline option glass for CEPC-HCAL. All the performance results of the scintillator glass in this new version, are the data of GFO.

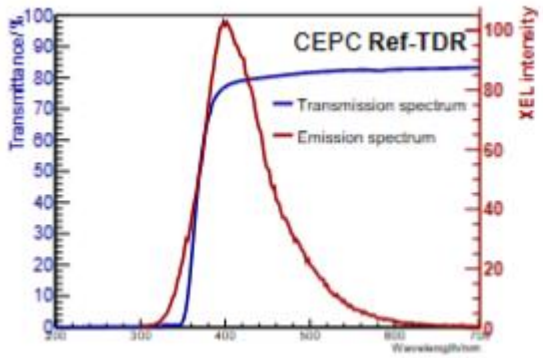

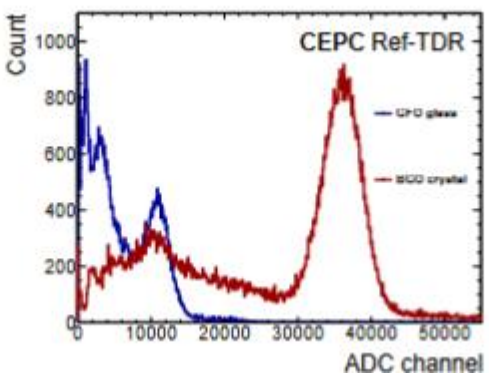

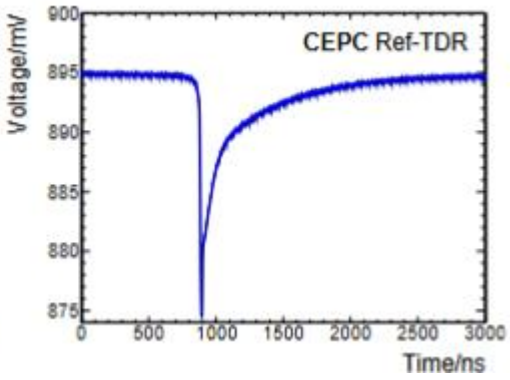

(a) Transmission and XEL spectra

(b) Energy spectra

(c) Scintillation decay curves

Comments

- A deep understanding of the response to hadrons is essential, including clarification of the constant term origin, study of the e/h ratio (software compensation), validation of GEANT4 physics lists, and accurate characterization of material properties such as quenching (Birks' law).

- --The new version of the TDR ahs already update the simulation work and the group also did more study for the design. In Section 8.5 simulation and performance. The energy linearity and resolution of the GS-HCAL are estimated using Geant4 simulation within the CEPC Software (CEPCSW) framework.

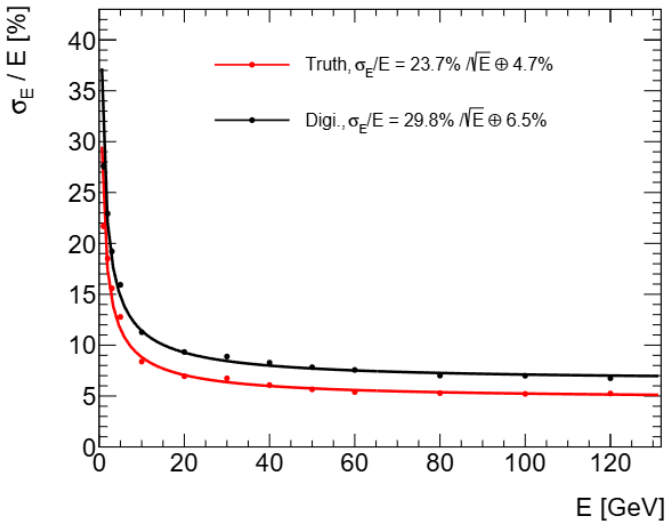

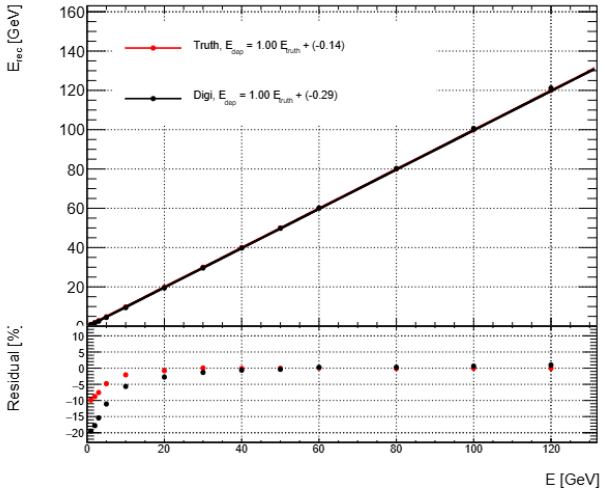

The estimated energy resolution of $\sigma E\ /E$ = 29.8%/$\sqrt{E}$ $\oplus$ 6.5% and an energy linearity within 2% before calibration, outperforms the stochastic term of traditional HCALs.

Comments

- The introduction of the TDR currently lacks references to important developments such as the CALICE AHCAL, built by German, Czech, and Japanese groups, which served as a foundation for the scintillator section of the CMS HGCAL.

- --The refs has already marked in the new version. Especially in the **Section 8.6** (Alternative HCAL options), it is introduced the developments of different option for HCAL. Multiple technological approaches of the CEPC calorimeters have been investigated to achieve the required jet energy resolution. While the baseline PFA-based GS-HCAL using glass scintillators offers superior performance, extensive R&D efforts within the CALICE collaboration have developed and systematically evaluated alternative solutions over the past two decades. These include gaseous detector-based approaches like the Digital HCAL (DHCAL) [29, 30] and SDHCAL [5, 31], as well as plastic scintillator tile designs (AHCAL) [10–13].

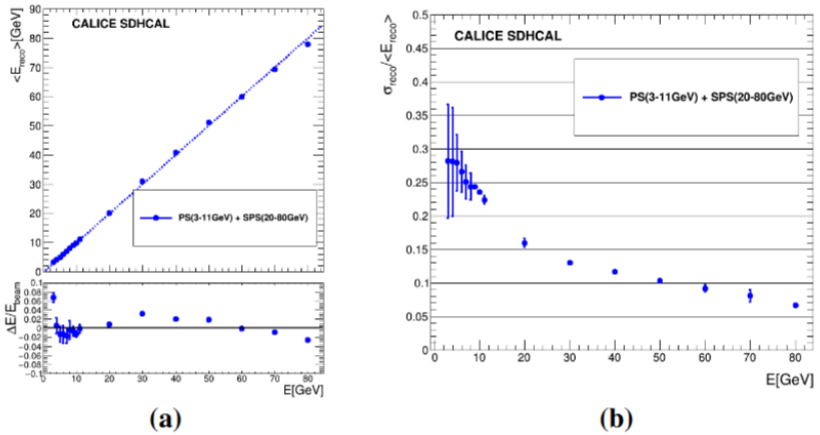

RPC-SDHCAL

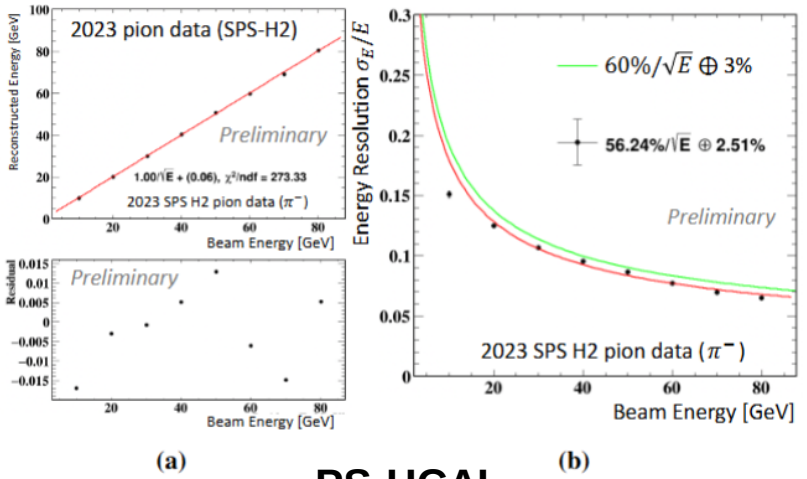

PS-HCAL

Comments

HCAL

- The process of down-selecting technology options should be better explained in the text. Statements such as "excessive power consumption" should be supported with quantitative arguments for clarity and transparency.

- --The quality of the language has already improved a lot in the new version. In this new version, only one person (Li Hengne) represents the whole HCAL team to write documents and hold discussions with others, maintaining the uniqueness of the writing style.

Recommendations

- Develop a detailed plan to validate the choice of GS-HCAL technology in a timely manner. This plan should include the development of glass samples with reproducible and controlled quality, along with a detailed understanding of single-particle and jet energy resolution.

- --Yes, in the new version, there is a new **section 8.4 (**Technology R&D to demonstrate technologies and prototypes) introduced the technology of HCAL as GS, SiPM, Simulation and Calibration. The evolution of glass scintillators in calorimetry reflects a series of iterative advances, from early exploratory designs to modern granular systems enabled by breakthroughs in photodetection and signal reconstruction. This section reviews the key milestones in glass-scintillator R&D, with particular emphasis on recent developments that have transformed their feasibility for large-scale HCAL. \

- In **Section 8.7** （Summary and future plan）described our plan for the GS-HCAL R&D. The baseline design, GS-HCAL, uses high density GS and SiPMs. It has a barrel and two endcaps, with a total of about 5.22 million cells, and is designed for PFA. The single layer structure consists of alternating glass scintillator cells and steel absorber plates, the barrel and endcap geometries are carefully designed for mechanical stability and efficient particle detection.

Recommendations

- Prioritize the construction of a full-scale prototype. This prototype should incorporate the preliminary selection of glass tiles and ideally include a first version of both the readout ASIC and the PCB. Decide early on the final configuration regarding the number of SiPMs per tile and implement this choice in the prototype.

- --Good suggestion, the final prototype will use the GS,ASIC and PCBs, which will be used in the HCAL-CEPC in the future. A 3×3×7 mini-prototype is currently under construction for initial beam tests at CERN in October 2025. This mini-prototype will use the DT5202 from CAEN (https://www.caen.it/products/dt5202/)for electronics. But the full 8112-channel prototype scheduled for completion by end-2026, with include the readout ASIC and the PCB by our electronics group in CEPC. The full 8112-channel prototype is scheduled for completion by end-2026, with cosmic ray tests planned at IHEP and subsequent beam tests preferably at CERN in 2027. This prototype implements a steel-scintillator sandwich structure in a compact 0.6 m^3 volume (52 cm × 52 cm × 130.6 cm).

- Organize the group's work such that the prototype is simultaneously implemented into the simulation framework, including a complete digitization chain, to enable rapid feedback from test beam campaigns.

- --Yes, These will be the next steps to focus on.

Comments in backup

HCAL

- As with other sections, the presentation was significantly better than the corresponding document and should serve as a guideline for revising the written material.
- -- the old version of the HCAL TDR has about 122 pictures and 70 pages, after the IDRC review, we have rewrite the new version with only 31 pictures and 40 pages without the reference.
- The authors are encouraged to make the text more concise where possible, while still providing sufficient detail where necessary.
  - o Captions such as that for Fig. 8.12 ("The real AHCAL prototype") are inadequate and should be made more informative.--the outline of the HCAL in new version has changed, this types of pictures were deleted.
  - o The authors should carefully review the text to ensure that all figures are properly motivated, and that the overall argumentation is logical and coherent.--the outline of the HCAL in new version has changed.
  - o For example, it is unclear why the emission spectrum shown in Fig. 8.52 is included—is it representative or used for digitization? This should be explicitly explained.--this figure was deleted. Totally about 91 figures aere deleted, and all the figures in the new version TDR were modfied with high quality.

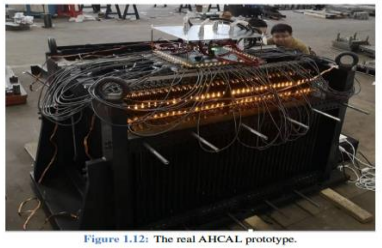

Fig. 8.12 in old version

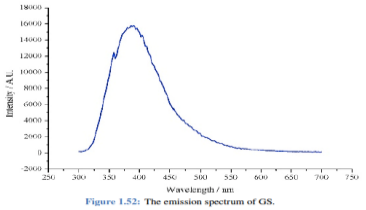

Fig. 8.52 in old version

Comments in backup

- The authors are encouraged to make the text more concise where possible, while still providing sufficient detail where necessary.
  - o In Fig. 8.45, while the test beam setup is now described, the reason for the visible shoulder (likely due to a double MIP peak) is not explained. Since the test beam is a major highlight of the R&D effort, the authors should focus on presenting it clearly and concisely, possibly selecting a few key highlights for emphasis.
  - --this part was rewrited as 8.4.2 Glass Scintillator --> Light Yield --> the MIP responce. Also the figure was changed as the new one **Figure 8.8.**
  - To evaluate the performance of Glass Scintillator (GS) dedicated beam tests and cosmic ray measurements were conducted, using 40×40×10mm3 GS tiles, and read out by SiPMs. The MIP response independently validated by the beam teat and the cosmic ray are consistence, in the **Table 8.4** Summary of GS tile beam test and cosmic ray measurements.

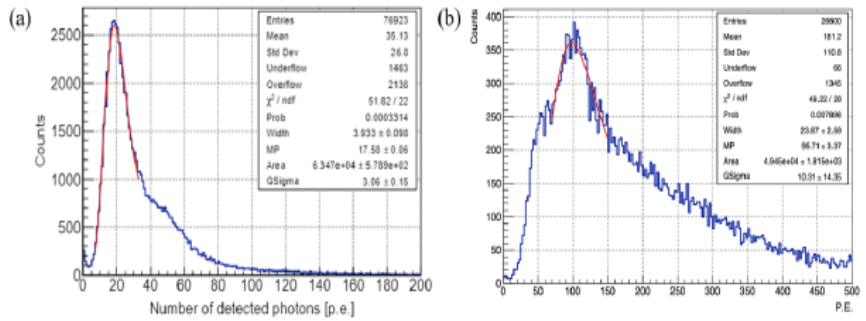

Figure 1.45: MIP response spectra of (a) #1 glass wrapped with Teflon tested by 10 GeV muon beam at CERN, (b) Quasi-MIP response spectrum for #4 glass scintillator tile tested by 5 GeV electron beam at DESY.

Fig. 8.45 in old version

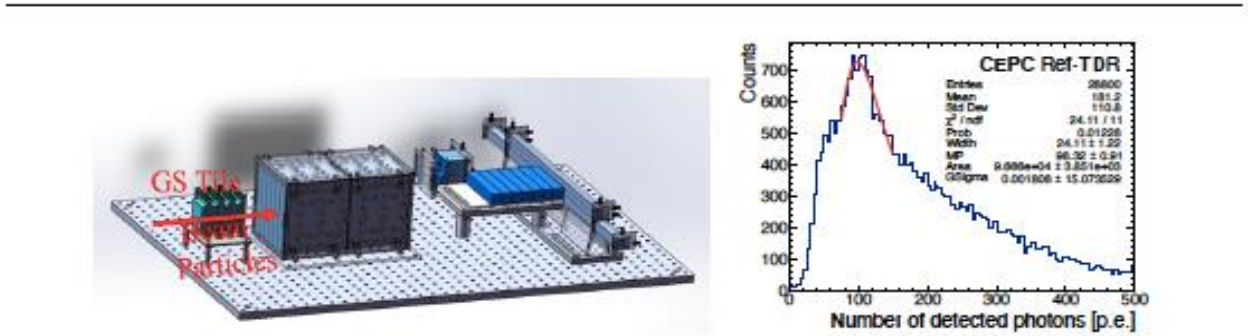

Figure 8.8: DESY electron beam test of the GFO glass tiles in 2023. Left figure shows the experimental setup, right figure shows the measured p.e. distribution.

Fig. 8.8 in new version

Comments in backup

HCAL

- Section 8.5 contains an extended discussion of SiPMs, mixing general background information with results from the collaboration's own R&D. This section should be streamlined to separate general background from specific experimental achievements.--.
- --this part was deleted in HCAL. The introduction of SiPM could be find in ECAL part. In the new version part, there is small **subsection 8.4.3** (Photon detector) anout the SiPM, as other key technologies include in the **Secion 8.4** (Technology R&D to demonstrate technologies and prototypes).

- Since SiPMs are used extensively across the calorimeter and muon systems, it would be more effective to consolidate the discussion of SiPM R&D into a single section. This would avoid redundancy and present a more coherent overview of the topic.
- --this part was deleted in HCAL. It could be find in ECAL part **Section 7.4.2** SiPM.

Comments in backup

- Mechanical integration aspects, currently occupying much of Section 8.7, could be better placed within a general "Detector Integration" section. The authors should use their judgment to decide which integration details are most relevant to retain in the specific HCAL section, while moving broader topics to a centralized discussion.
- --there is the new section about the mechanical part at the begin of the HCAL as 8.2 Design part. The Outline of the HCAL part are the same an other Detector, first the design, then the Key technologies, both the major challenges and the R&D results. Then the simulation and performance. The Alternative HCAL options are to be a special section to overview the other group's work for the HCAL.

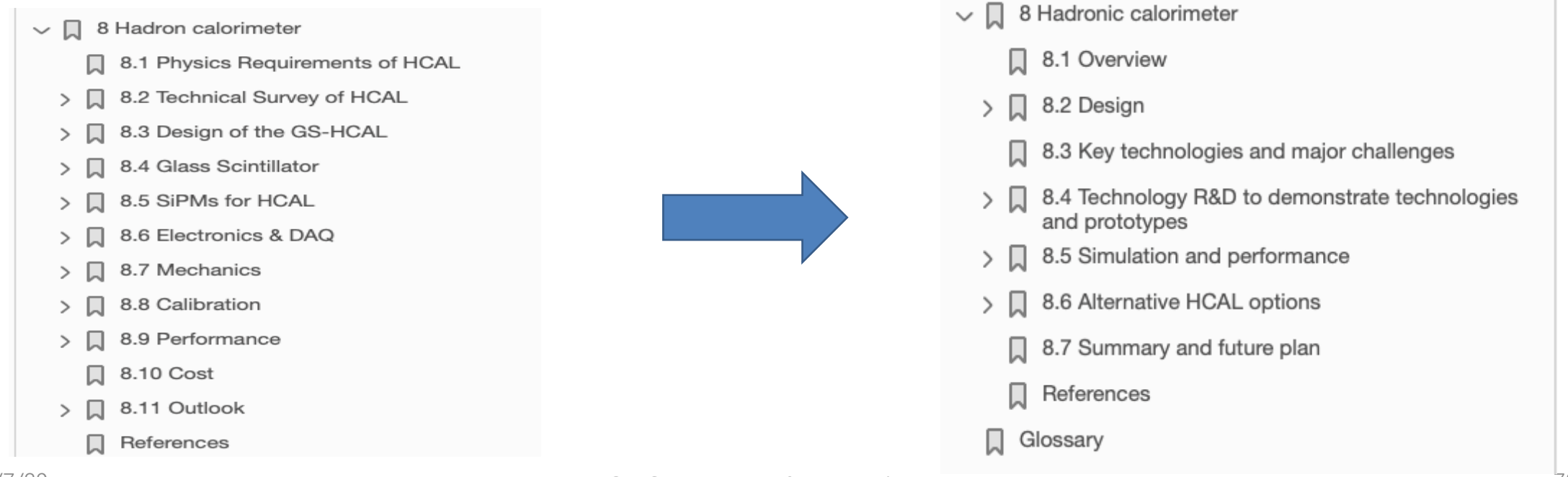

Comments on Draft v0.4

- General comment
- Let us first congratulate them for the huge amount of interesting work that is presented. As already observed for the Eca part also the HCal part has been restructured. It also presents directly the design choice and comments on alternatives at the end of the chapter, meeting therefore a comment made during the review in April. In the following a few high level comments and a non-exhaustive list of line-by-line comments. An annotated pdf file of the HCal put has been put at the disposal of the project members.

Comments on Draft v0.4

- High-level comments
  - Still the main problem is that a technology is proposed that is at the very beginning of the R&D cycle
    - ○From our point of view It will take at least five years with full resources before this calorimeter will reach the TDR level
    - ○We note however that the authors show awareness of this (major) shortcoming
    - ○The project matches perfectly a strategic R&D topic in DRD Calo but is too early for a TDR.

--we should try our best to write this document as the part of the Ref-Detector-TDR of CEPC.

1） several components of the is technology are similar to ones used in the AHCAL technology like SiPM and readout systems as well as calibration techniques. All this is integrated in the new technology

2） although future extensive tests will confirm it, the simulation used to produce the TDR results seems to be corroborated by the first beam tests and cosmic benches.

3) the strong collaboration with local industries allow us to be confident that new generation of scintillanting glass will provide even higher performances in terms of light yield and attenuation length leading to even much better performances than the ones put in the TDR.

○How critical is the non availability of CERN (i.e. a high energetic hadron beam) between the middle of 2026 and ~2029.

---May be in KEK or the Proton beam in CSNS in China.

Comments on Draft v0.4

- High-level comments
  - The document lacks a clear plan toward construction

  --please see the section 8.5.8 Prototype, the section 8.8 Summary and Future Plan.

  - What are design parameters (on e.g. cell S/N) of the system?

  --please see the section 8.2.1 Single Layer Structure.

  - At the moment only a handful of tiles have been tested
    - How to ensure mass production?
    - In this context how to ensure homogenous tiles and what are the criteria?

    --No matter what. We must trust the production capabilities and quality control of Chinese enterprises.

    --the successfull example is the 20 inch MCP-PMT for JUNO. We get the small number of prototypes at Lab in 2015, and the factory setup the mass production line in 2016, and start the mass production from 2017 to 2020, finished 15000 pics 20 inch MCP-PMTs for JUNO.

    --for the Glass Scintiallator and SiPM, the situation right now are really much better than the PMTs at that time. When the CEPC will be supported by the goverment, the factories will do the mass production by themeslves.

Comments on Draft v0.4

In the draft we don't see the results of all the (few) tiles that have been e.g. tested beam or in the cosmic stand

--In Fact， in the Section 8.4.5 Measurements of GS with SiPM, the Figure 8.13: Measured ADC spectrum of GS cell with a SiPM (HPK S14160-3050HS) using 137Cs radiative source. Figure 8.14: Cosmic ray test results of the GS tile measured using SiPMs.

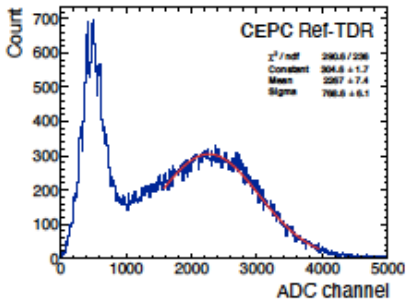

Figure 8.13: Measured ADC spectrum of GS cell with a SiPM (HPK S14160-3050HS) using ^{137}Cs radiative source.

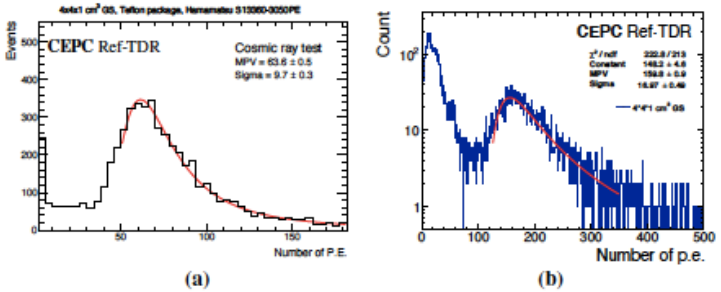

Figure 8.14: Cosmic ray test results of the GS tile measured using SiPMs. The same GS tile with a size of $40mm \times 40mm \times 10mm$ is used. (a) The measurement at SJTU measured using Hamamatsu S13360-3050PE SiPM, resulting a light output about of 64 p.e./MIP. (b) The measured result at IHEP of a value about 160 p.e./MIP using a Hamamatsu S13360-6025CS SiPM. The two results are consistent. The difference is due to the different sizes of the SiPMs, and different PDEs.

- There are inconsistencies; examples (non exhaustive)
  - All SiPM tests in 8.4.4 were carried out with HPK SiPMs however for the prototype NDL SiPMs will be used

    --all changed, not fix the SiPM for HCAL.
  - Is the pre-amp tested in Sec. 8.4.6 the same that will be used in SIPAC?

    --not yet. The pre-amp was combined in ASIC, which has not designed for using right now.

Comments on Draft v0.4

- On Page 290 the authors raise concerns about the radiation hardness.
  - The tiles will not withstand 10 years of operation. Is this a fundamental problem and if yes how will this be systematically addressed?

  --indeed, you correctly pointed out adiation hardnes is not a fundamental problem. Previously we spent many text discussing radiation damage but in fact it is not really an issue. We have receved comments from several experts that the radiation damage is actually not an issue in electron-positrom machine such as CEPC, we agree on that and re-evaluated the situation, we deceided to remove a large fraction of the radiation damage discussion.

- The description of the cooling system (Page 279) is insufficient.

-- agree, adding more text and a figure to better describe the cooling system. More detialed could be seen in Section 8.2.2 Barrel and Section 8.2.3 Endcap.

Comments on Draft v0.4

- Think to shorten the introduction to 8.4
- --The Part 8.4 have to change as follows:
- keep the 8.4.1 Historical review; 8.4.3 Photon detector; 8.4.6 Calibration;
- 8.4.7 Readout electronics for R&D; 8.4.8 Prototype

- rename 8.4.4 Simulation study of attenuation length as 8.4.4 Simulation study of Glass Cell;
- rename 8.4.5 Measurements of GS with SiPM as 8.4.5 Cosmic Ray Test of the Glass Cell

- **rewrite the 8.4.2 Glass scintillator;**

(1) light yied, (2) Light attenuation length; (3)Radiation resistance

- **rewrite the 8.4.2 Glass scintillator; (1) light yied,**
- delate the result of the electron beam result;
- remove cosmic ray test result to 8.4.5 Cosmic Ray Test of the Glass Cell

Light yield

Figure 8.6 shows the photograph of GFO glasses with $40\times40\times10$ mm^3 under natural and ultraviolet light. Extensive γ-ray testing has demonstrated that the light yield of GFO glasses can consistently exceed 1000 ph/MeV. When measured with an XP2020 PMT, the detected photo-electron number reaches 1/3 that of BGO crystals with identical dimensions, as shown in Figure 8.7(b). Figure 8.7(c) presents the scintillation decay profile

12

of GFO glass under γ-ray excitation. While maintaining a light yield of 1000 ph/MeV, the decay time of the slow component can be controlled to below 500 ns. Although achieving faster decay time remains challenging, the large-scale GFO glass successfully maintains an optimal balance between density, light yield, and scintillation decay characteristics.

Figure 8.6: GFO glass tiles of the size $40\times40\times10$ mm^3 under natural light and ultraviolet light.

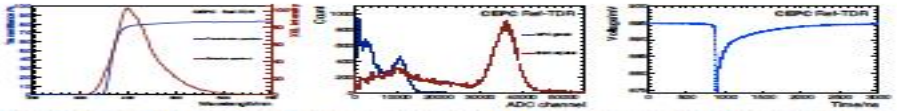

Figure 8.7: (a) Transmission and X-Ray Excited Luminescence (XEL) spectra of large GFO glass, (b) Energy spectra of GFO glass scintillators and BGO crystal with same dimension. (c) Scintillation decay curves of GFO glass

However, as illustrated in Figure 8.7 (a), these glasses still exhibit strong self-absorption in the ultraviolet spectral region. Additionally, as the glass thickness increases, its transmittance in the visible spectrum decreases from approximately 80% to around 75%. The measurable light output of GFO glass became a critical factor for HCAL applications.

To evaluate the performance of Glass Scintillator (GS) dedicated beam tests and cosmic ray measurements were conducted, using $40\times40\times10$ mm^3 GS tiles, and read out by SiPMs.

Nine GS tiles were exposed to 5 GeV electron beam at the Deutsches Elektronen-Synchrotron (DESY) test facility. The acquisition system was configured with an integral gate of 1 μs to capture the scintillation signal, reading out using Hamamatsu S13360-6025PE SiPM. The Photoelectron (p.e.) spectrum showed a Most Probable Value (MPV) of approximately 90–100 p.e./MIP. The measured light yield was in the range of 600–700 photons/MeV, consistent with expectations for high-density GS tiles. The setup is illustrated in the left panel of Figure 8.8, with the corresponding p.e. spectrum shown on the right side.

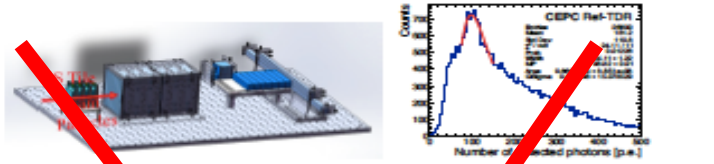

Figure 8.8: DESY electron beam test of the GFO glass tiles in 2023. Left figure shows the experimental setup, right figure shows the measured p.e. distribution.

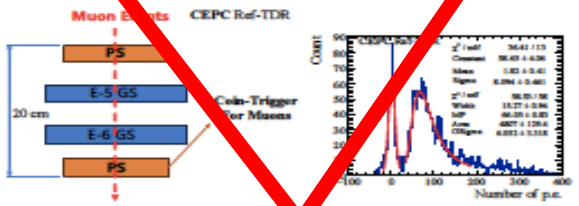

Figure 8.9: IHEP cosmic ray setup performed in 2024 of GFO glass tiles (left), and the measured p.e. distributions for MIPs (right)

To independently validate the MIP response, a second measurement was performed using cosmic muons in a vertical stack configuration at IHEP in 2024. Two Plastic Scintillator (PS) paddles provide coincidence triggers above and below the GS tiles (labeled E-5 and E-6) to ensure clean muon tracks. This setup is schematically shown in the left panel of Figure 8.9. The readout is using Hamamatsu S13360-6025CS SiPM. A longer integral gate of 4 μs was employed to fully collect the slower scintillation components. The measured MIP response of the E-5 tile reached an MPV of approximately 67 p.e./MIP, corresponding to an inferred light yield of ~750 photons/MeV, which is consistence with the DESY results.

Both measurements confirm the feasibility of using GS tiles for high-granularity HCAL applications. A summary of the results is presented in Table 8.4. These results validate the promising performance of GS tiles and provide critical input for optimizing the calorimeter design for CEPC.

Table 8.4: Summary of GS tile beam test and cosmic ray measurements

Test Setup	Integral Gate	Light Yield	MIP Response
DESY Electron Beam	1 μs	600–700 ph/MeV	90–100 p.e./MIP
IHEP Cosmic Ray (E-5)	4 μs	~750 ph/MeV	65–70 p.e./MIP

- **rewrite the 8.4.2 Glass scintillator; (2) Light attenuation length,**
- delate the test result of the data by the light output in our lab published in Ref[18];
- retest the samples by the transmittance data and give the new results and also the ref.？ .

Light attenuation length

The attenuation length (L_0) is a critical parameter for evaluating light transmission performance in scintillators. Multiple batches of GFO glass samples with cross-sectional dimensions of $5 \times 5\,\mathrm{mm}^2$ and thicknesses ranging from 1–15 mm were prepared for systematic measurements (Fig. 8.10). The best-performing GFO glass sample currently available achieves an attenuation length of 6.2 cm at 400 nm. This value is used as the standard reference in the TDR, and all performance results are based on it.

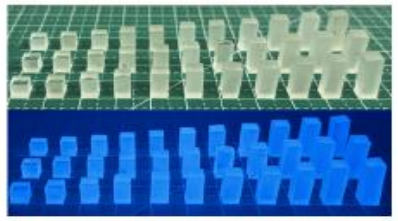

Figure 8.10: GFO glass samples under natural light (top) and ultraviolet light (bottom).

The light attenuation follows the exponential relation is given by $Y = Y_0 \cdot \exp(L/L_0)$, where Y_0 is the initial photon yield, Y the yield after propagation distance L, and L_0 the characteristic attenuation length. Initial measurements yielded $L_0 = 2.3 \pm 0.01$ cm [18], limited by glass matrix defects and Ce^{3+} self-absorption.

Through process optimization, the light yield of GFO glass increased from 1000 to over 1500 ph/MeV, suggesting corresponding attenuation length improvements. Figure 8.11 (a) illustrates the γ-ray spectral method for determining the light attenuation length. The method involves measuring the ratio of the initial light yield (Y_0) to the light yield after transmission through varying glass thicknesses (Y). By fitting this ratio as a function of thickness, we extract the attenuation length, yielding a value of $L_0 = 2.3$ cm and $L_0 = 3.4$ cm for two batches of glass samples before and after optimization, respectively.

A more accurate method determines L_0 through thickness-dependent transmittance (T) can be written as $L_0 = (L_2 - L_1)/\ln(T_{L_1}/T_{L_2})$, where T_L is the transmittance at thickness L. This method accounts for full-volume light penetration, eliminating position uncertainty. Figure 8.11 (b) shows the improved attenuation length of 6.2 cm at 400 nm (emission peak), with consistent 5.8–6.2 cm performance across the visible spectrum - a 100% improvement over previous samples (3.1 cm at 400 nm). These results confirm that γ-ray methods systematically underestimate L_0, while verifying GFO's about 6 cm attenuation length enables efficient light collection.

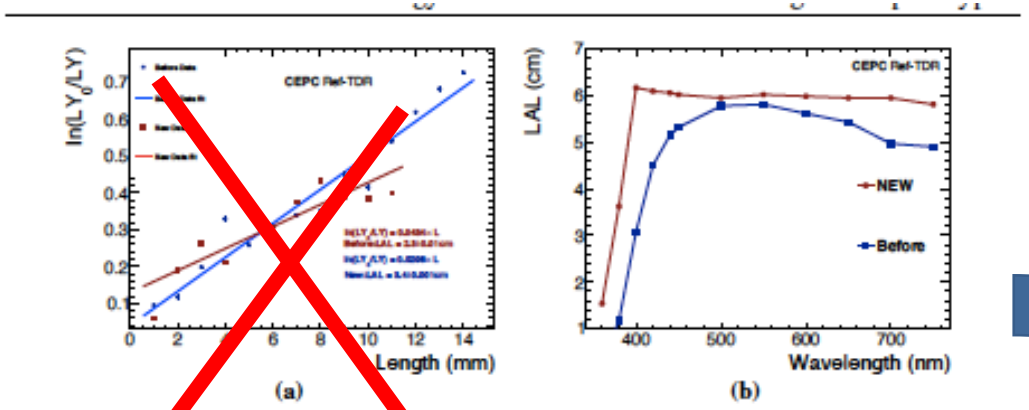

Figure 8.11: (a) Light yield ratio $\ln(Y_0/Y)$ as a function of the thickness of the glass is fitted to extract light attenuation length (LAL). (b) Attenuation length spectrum from transmittance measurements ("New": current GFO; "Before": previous samples).

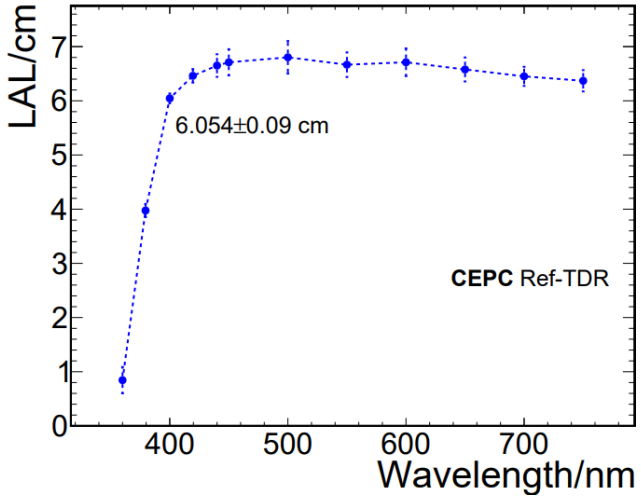

- **rewrite the 8.4.2 Glass scintillator; (3) Radiation resistance ,**
- just delate this part and give the result in (1) Light Yield part. and ref the papaer published in NIMA about this result right now (suggested by lmad).

Radiation resistance

The radiation resistance of glass scintillators is crucial as their performance degrades after irradiation. The GFO glass samples were studied using an 80 MeV proton beam at the Associated Proton Beam Experiment Platform (APEP) [19] across a wide dose range (400 Gy to 4.1×10^4 Gy). Proton flux for this test is 4.86×10^9 (p/cm²/s), and the beam spot size is 50×50 mm². Seven $5\times5\times10$ mm³ pieces (labeled #1–#7) were used for this test, using different radiation time to obtain corresponding radiation dosage as shown in Table 8.5). Sample #1 kept as an unirradiated reference.

The scintillation properties were characterized through transmission spectra, XEL, light output, and decay time measurements (Table 8.5). Unirradiated sample showed 78% transmittance at 400 nm, while transmittance of irradiated samples dropped to 31% with a dose of 800 Gy, and further dropped to 10% for a dose of 8100 Gy, consistent with visible color changes indicating defect formation. The Ce^{3+} emission peak (386 nm in unirradiated samples) shifted slightly to 376–384 nm after irradiation. Figure 8.12 displays the visual changes in samples #1 to #7 under progressively higher radiation doses, with increased dosage correlating to decreased transparency and darker color.

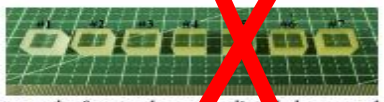

Figure 8.12: The photograph of proton beam irradiated glass samples. From sample #1 to #7, the radiation dosage progressively increases, resulting in darker color with decreased transparency.

In contrast to proton irradiation, gamma irradiation tests evaluate performance degra-

16

8.4 Technology R&D to demonstrate technologies and prototypes

Table 8.5: Performance summary of the glass tiles after proton irradiation test.

Sample	Dose (Gy)	Transmittance @ 400 nm (%)	XEL (nm)	Light Output (ph/MeV)	Decay Time (τ) (ns)
#1	0	77.9	386	552	87, 985
#2	400	37.4	376	187	89, 980
#3	800	31.3	380	–	–
#4	2000	13.7	384	–	–
#5	4100	10.4	376	–	–
#6	8100	8.3	380	–	–
#7	41000	5.8	376	–	–

dation at lower doses (10–400 Gy). A ^{60}Co point source (3.656×10^{11} Bq) was used, emitting gamma rays at 1.1732 MeV and 1.3325 MeV. The absorbed dose rate follows the inverse square law relative to the source distance. Six $5\times5\times5$ mm³ glass samples were irradiated simultaneously for 37.5 hours at varying distances (10–63 cm) to achieve different dose rates, slight yellowing (darkening in color) for samples with higher radiation dosage can be observed.

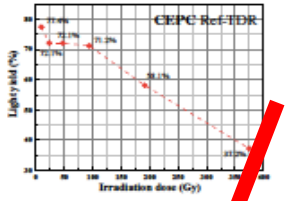

Figure 8.13: Gamma irradiation results showing the relative light yield of the scintillator as a function of irradiation dose. The light yield decreases gradually with increasing dose, reaching 71.2% at 100 Gy.

Scintillation performance was characterized through transmission spectra, XEL, light output, and decay time measurements. The maximum transmittance degradation was 14% - significantly less severe than proton irradiation at comparable doses (400 Gy). This difference likely stems from the lower dose rate and reduced ionization damage in gamma irradiation, as protons have higher linear energy transfer. The emission peaks remained stable (380-386 nm), consistent with proton irradiation results. Light output measurements using the same ^{137}Cs/PMT setup showed progressive degradation: 71% retention at 100 Gy and 37% at 375 Gy, matching proton irradiation trends. Decay times exhibited minimal variation, 87-89 ns fast component, 978-985 ns slow component, again consistent with proton irradiation observations. The gamma irradiation test results of the scintillator samples, showing the relative light yield as a function of accumulated dose, are shown in Figure 8.13. A significant degradation in light yield is observed with increasing dose,

17

8.4 Technology R&D to demonstrate technologies and prototypes

with the yield dropping to about 71.2% at 100 Gy. This corresponds to an expected total dosage (about 100 Gy of CEPC HCAL after 10 years of data taking.

The comparative analysis reveals that while both radiation types cause similar qualitative effects, gamma irradiation induces less severe degradation at equivalent doses. This suggests that the damage mechanism depends not only on total absorbed dose but also on radiation type and dose rate, with proton irradiation causing more severe ionization damage due to higher linear energy transfer.

Comments on Draft v0.4

- The constant term is still an issue.
  - Line 7867: "Both approaches led to a reduction in the fitted constant term". What was the fraction of the events that were selected?
  - We propose to show the linearity in addition to the resolution
  - Please comment on the expected e/h ratio
  - We understand "all inner sub-detectors are removed" in this study.
  - Since there will be an ECAL before the HCAL in the actual experiment, the effective depth of calorimetry will be larger and the selection and constant term (with and without selection) will be different. It is also interesting to investigate how the different responses in the ECAL and the HCAL will impact the constant term in the integrated detector.
  - The AHCAL prototype discussed in Sec. 8.6.2 has a depth (from memory) of 4-5 interaction lengths but a constant term of only 2.59%. Thus, the depth cannot be the only reason for the large constant term of the GS HCAL

  --Agree, we agree with your suggestions above, we are implementing them one by one, as you have correctly pointed out, this section needs much more work with careful thinking to improve.

Comments on Draft v0.4

- Line-by-Line Comments
- Line 6952 - "The HCAL is a key component in achieving the jet energy resolution". One may could argue it is THE key component
- Lines 6962-6964 "plastic scintillators and gaseous detectors, with readout based on SiPMs or other photon sensors.". This is confusing. Maybe "plastic scintillators, with readout based on SiPMs or other photon sensors, and gaseous detectors."?
- Line 6983 "$W$and Zdecays" - spaces missing - "W and Z decays"
- Lines 7042-7043: "851.34 mm" and "1367.56mm" are unnecessarily precise (10 microns).
- Could this be rounded off to mm?
- Figure 8.3: "851.34 mm" and "1367.56mm" are unnecessarily precise (10 microns). Could this be rounded off to mm?
- Lines 7570-7574: Could some example distributions be shown?
- Line 8066 "measure hadronic jets energy" I believe jet should be singular. "measure hadronic jet energy" line 8068 "GS and SiPMs'. We suggest spelling these out again when first mentioned in the summary
- Line 8082 "This can be achieved" -> may be achieved? -> "This may be achieved"

---Agree, the pointed out parts have already update in the new version.

MUON

Findings

- The TDR presents a baseline design for the Muon Detector based on extruded plastic scintillator (PS) bars, coupled with WLS fibers and SiPMs. This approach is cost-effective, and the primary objective is to demonstrate that the system can meet stringent performance requirements across the detector's large active area.

- The Muon Detector will consist of six superlayers in both the barrel and endcap regions. It uses long scintillator strips, 4 cm wide, with lengths exceeding 4 meters. Due to WLS fiber routing, effective optical lengths can be even longer, making attenuation length a critical parameter, directly impacting timing resolution and detection efficiency. Enhanced light collection strategies are thus essential.

- The readout system adapts designs from the ECAL and HCAL and includes uSiPMs, front-end boards (uFEBs), and management boards (uMBs), tailored specifically for the Muon Detector. 14 Background studies show a maximum hit rate of ~2 Hz/cm², comfortably below the system's rate capability.

- The Muon Detector supports trigger functionalities, including tagging long-lived particles (LLPs), although integration into the full CEPC TDAQ system remains preliminary. RPC technology, using environmentally friendly gases, is also under consideration via the DRD1 collaboration.

Comments

The TDR chapter and the review presentation show significant technical progress with clear physics motivation and encouraging prototype results. However, several areas need further development:

- Testing of full-length bars (4.2–5 m) must be completed, fully implementing optimized light collection methods.
- Standardized procedures for optical glue application (thickness, curing time) and validation of coating quality at scale are still required. A detailed system-level comparison between NDL and MPPC SiPMs is lacking. Given the Muon Detector's lower light yield and tighter timing requirements compared to calorimeters, selecting the optimal SiPM is critical.
- Consolidated detector specifications (spatial and time resolutions) must be validated through simulations and trigger performance studies

Recommendations

MUON

- Complete comprehensive tests on full-length bars using final SiPM configurations and 2.0 mm WLS fibers, measuring timing, light yield, and efficiency.
- Two 4-m strips using EQR-15 SiPM and 2.0 mm WLS fibers were tested, with timing, light yield, and efficiency reported in the new version.
- Define standard application procedures and conduct studies addressing mechanical stability, aging, radiation resistance, and refractive index.
- This part is not included yet.
- Systematically assess MPPC and NDL SiPMs (including new 20 μm pixel versions), focusing on gain, DCR, cross-talk, and operating thresholds under realistic conditions.
- Comparison of the two SiPMs are included in Sec. 9.3.2, but no 20 μm pixel versions. Suggest add a table for better comparison. More studies are needed for the SiPM selection.
- Expand simulation studies to include full event samples, especially displaced vertex signatures, to validate and refine time resolution requirements. I
- t is difficult for me find out the simulated event samples as they are not introduced in the beginning the simulation section. Single muons and pions with different momentum are simulated as I can tell.
- Clearly state detector performance requirements linked to physics goals. Move Muon ID algorithm discussions to the global TDR Performance chapter and focus this chapter on local and standalone performance. Ensure consistent technical terminology and improve figure referencing.
- Efficiencies of muon and pion are introduced in the current version.

Findings on Draft v0.4.1

- The updated Muon Detector chapter in the CEPC Reference TDR (Barcelona version) shows clear improvements over the previous iteration:
  - The chapter is better structured and easier to navigate.
  - A performance summary table is now included early in the chapter.
  - Key technologies—such as SiPMs, long scintillator strips, and optical coupling—are described more clearly.
  - The new EQR-20 SiPM (20 μm pixel, higher gain, lower DCR) is introduced, and preliminary test results are presented.
  - Initial prototype results for long strips (up to 4–5 m) are now included.
- These updates are welcome and demonstrate tangible progress. However, several important technical and editorial issues remain only partially addressed or unresolved.

Comments on Draft v0.4.1

1. Long-bar prototype test results

- The inclusion of tests for 4–5 m strips is a positive step, but the presented information lacks clarity and context.
- Figures (e.g., Fig. 9.12) are not well integrated into the text and sometimes captions are confusing.
- The intended target threshold remains undefined, despite reporting signal yields at various p.e. levels.
- Results from IHEP and Fudan differ in setup (SiPM type, fiber), and the comparison lacks explanation.
- Dual-ended readout is briefly mentioned but not quantified or discussed.

2. SiPM characterization (NDL vs. MPPC)

- While pixel size and gain differences are noted, the comparison remains superficial.
- Critical performance aspects—such as timing, noise, cross-talk, and behavior under temperature or radiation—are not evaluated.
- There is no final decision or validation plan for SiPM selection.

3. Readout architecture and threshold definition

- The readout chain is inherited from ECAL/HCAL but lacks justification for its use in the Muon Detector.
- Lower light yield and tighter timing constraints raise concerns about its suitability.
- Thresholds shown in figures are not linked to a defined operating point or noise model.

Comments on Draft v0.4.1

4. Trigger strategy

- Trigger concepts are mentioned (e.g., LLP tagging), but no logic, architecture, or latency assessment is included.
- No integration plan with the CEPC trigger system is presented.

5. Simulation studies and background

- Beam background simulations are provided and show manageable occupancies.
- Section 9.4.3 suffers from language issues (tense shifts, awkward phrasing).
- No physics-driven simulation studies (e.g., low-pT muons, displaced vertices) are presented.
- Detector performance specs (e.g., timing, granularity) are not explicitly linked to physics goals.

6. Structure and editorial issues

- Figure referencing is sometimes incomplete.
- Section 9.3.3: The last paragraph of this section is duplicated, likely due to a copy-paste error. This repetition should be removed. In addition, the text would benefit from a general language revision to fix grammatical issues (e.g., subject-verb agreement, article usage) and improve clarity.
- Section 9.4.3: The background paragraph conveys relevant information, but the English requires significant improvement. Verb tenses are inconsistent, and some expressions are unclear or incorrect. A thorough revision is needed to improve clarity and readability.
- Terminology and language quality vary across the chapter and require final editorial revision.

Recommendations on Draft v0.4.1

Considering that the TDR is near completion, we do not expect extensive new studies. Nonetheless, to improve clarity and completeness, we recommend:

Clarify prototype study objectives

- Explicitly state the performance targets (e.g., threshold, signal yield, efficiency, timing) for long-strip tests and explain how the results support detector requirements.
  Threshold and noise strategy
  Even if a final threshold is not yet fixed, describe the criteria and expected noise level. Justify the thresholds used in figures and explain how they relate to realistic detector conditions.

Readout chain evaluation

- Acknowledge the differences between the Muon and ECAL/HCAL environments. Outline how the current electronics will be validated or adapted to meet the Muon Detector's demands.

SiPM selection process

- Describe the performance metrics which will drive SiPM selection (e.g., dark noise, gain, radiation tolerance) and outline upcoming R&D needed for final validation.

Trigger implementation

- Provide at least a minimal scheme and indicate how integration with the CEPC trigger system will be assessed.

Simulation roadmap

- Include plans to simulate full physics events and connect detector specs to the physics motivation (e.g., LLP, muon ID performance).

Final editorial revision

- Ensure all figures are referenced in the text, remove the duplicated paragraph in Section 9.3.3, and revise language in Section 9.4.3 for clarity.

SUPERCONDUCTING SOLENOID

Findings

- The CEPC Ref-TDR superconducting solenoid design has made significant progress. The solenoid provides a central magnetic field of 3T (for $t\bar{t}$, Higgs, and W runs) and 2–3T (for Z runs), with an inner bore diameter of 7.07 m and a cryostat/yoke half-length of 4.53 m. It is enclosed within an iron yoke that also houses the muon detector. The variation of the solenoid magnetic field in the central tracker (TPC) region is currently calculated to be approximately 10%.
- The solenoid coil design is based on four layers of Al-stabilized superconductor, supported by an aluminum-alloy outer support cylinder and cooled using a two-phase helium thermosiphon system. This general design concept is well established, drawing on the reliable design experience of the CERN-LHC CMS detector.
- A key technology development effort focuses on Al-stabilized superconductors, with two approaches to mechanical reinforcement:
  - Option A: Double-layered, two-step co-extrusion process.
  - Option B: Single extrusion with micro-alloying for reinforcement, followed by a cold-work process.
- Further R&D is planned for 2025.
- The maximum von Mises stress on the Al-stabilizer during magnet excitation is evaluated at 96 MPa, which is close to the current yield strength of the Al-stabilizer material (105 MPa). Further mechanical evaluation is necessary to ensure an adequate safety margin, including the mechanical integrity of the NbTi/Cu superconductor itself.
- Remaining technical challenges primarily concern the production of large-scale, high-strength Alstabilized superconductors, as well as ensuring the reliability of the numerous aluminum-pipe welds required in the thermosiphon cooling system

Comments

- Field uniformity in the TPC region is a fundamental boundary condition for detector performance. The current 10% field variation must be carefully assessed to ensure it is acceptable for the required TPC performance. It is important to note that the ALICE detector has a different configuration, and that the ALICE magnet is much larger resulting in significantly better field quality in its TPC region compared to CEPC.

Impact on tracking:

- It is impossible to achieve a uniform magnetic field in the experiment. Fortunately, the impact of non-uniform magnetic field on the momentum measurement can be minimized if the track fitting algorithm (i.e. Kalman filter) can deal with the non-uniform magnetic field with the measured magnetic field map.

The key issue is whether we use a right field map in software. Two requirements

- Measurement precision of the magnetic field map is good enough.
- Gradient of the field small enough (The map is smooth, without big fluctuation within small area)

CEPC magnetic field gradient of the TPC region:

The gradient of TPC region is around $5.4*10^{-5}$ T/mm, which is small enough and meets the requirement

Measurement precision:

If the measurement precision is 10^{-3} (i.e., position error during measurement is around 1mm), the deviation of B is around $5.4*10^{-5}$ T according the gradient, which meets the requirement of momentum resolution (~0.1%)

An example of BESIII

- NUMF in BESIII is 5%, and measurement error of B is around 0.3%
- The momentum resolution is good as the expected after the track fit with Kalman filter and track-based calibration. No significant impact from NUMF is observed.

Comments

- The committee recognizes the remarkable progress achieved in developing Al-stabilized superconductors, achieving a yield strength of 105 MPa at 4.2 K using micro-alloying (Ni + Be). However, further R&D is required to demonstrate the full mechanical performance of the conductor and the successful fabrication of full-scale Al-stabilized superconductor segments.
- It is critical to demonstrate that the full conductor (NbTi/Cu + Al-stabilizer) can withstand mechanical stress up to 135 MPa. This threshold is about 50% higher than the maximum von Mises stress (~90 MPa) expected during operation at 3T. If achieving this mechanical strength proves difficult, increasing the thickness of the support cylinder could be considered, although this would be undesirable. As a last resort, if necessary, a reduction in the operating field strength may need to be discussed.

The stress issue can be addressed by either increasing the cross-sectional area of the aluminum stabilizer or enhancing the yield strength of its material. However, due to the current limitations in the size of the aluminum coating equipment and the overall design dimensions of the detector, it is relatively difficult to increase the cross-sectional area of the aluminum stabilizer. We made certain progress in the development of Box type conductor, which has a better mechanical performance. We will continue to do the R&D of high strength and RRR value aluminum stabilizer.

Secondary co-extrusion **Box type** Cable size and structure: **56mm*22mm (Box type)**

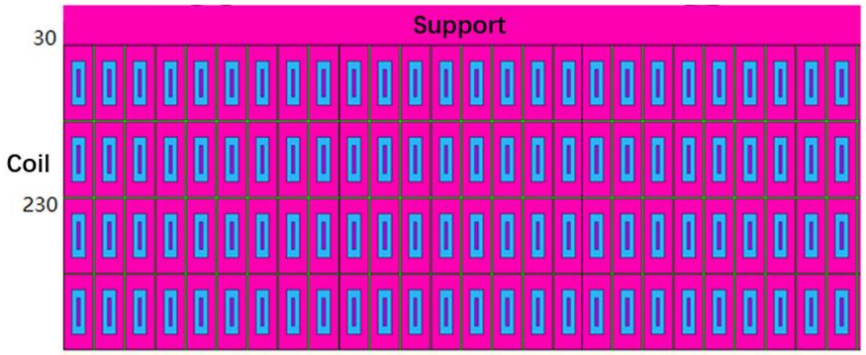

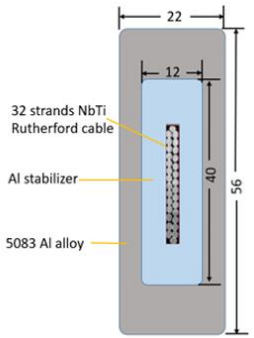

Material	Von Mises stress (MPa)	Von Mises strain (‰)
	Coil at 4.2 K	
Aluminum stabilizer	7.7-20.0	0.1-3.01
NbTi/Cu cable	177-279	1.36-2.15
Al alloy	7.0-43.3	0.05-0.1
Al alloy support	6.3-36.3	0.1-0.44
	Coil at 4.2 K, energized	
Aluminum stabilizer	14.3-22.5	0.85-4.09
NbTi/Cu cable	28-246	0.2-1.9
Al alloy	60.8-137	0.7-1.7
Al alloy support	62.2-127	0.7-1.57

Comments

- Developing a scaled model coil, including full cooling and excitation tests, will be an important step. Without such a demonstrator, confidence in the readiness of the solenoid technology for CEPC will be limited.

Establishing a scaled model coil is really a necessary step before the processing of the detector magnet, and we will take this important process into consideration in our subsequent planning.

- Two cooling channel designs are under consideration:
  - Vertical Al-pipe channels, as used in CMS.
  - Sloped or tilted serpentine channels, which may reduce the number of welds and save cryostat space.
- The latter option could be advantageous for construction reliability

Thank you very much for your excellent suggestions. We will optimize the cooling system from two aspects: Design and Welding Technology

(1) We will consider doing the design of the sloped serpentine cooling path, on one hand, meets the requirements of temperature distribution, and on the other hand, reduces the number of welds.

(2) Regarding the welding of aluminum tubes, we had experience in welding small model coils, but we have not yet had experience in welding such a large number of pipes in a large-scale cooling structure. We will conduct verification experiments in the near future.

Recommendations

- Carefully verify that the magnetic field uniformity of the CEPC Ref-TDR solenoid meets the TPC performance requirements without introducing unacceptable distortions to particle drift paths. If the current configuration proves insufficient, consider alternative design modifications—such as the addition of compensation windings in the forward and backward regions, as explored in ILD studies, or adjustments to the shape and configuration of the magnetic iron poles.

We will carefully verify the magnetic field uniformity with TPC collogues, put the simulated magnetic field distribution into TPC simulation software.

- Maintain the highest priority for the R&D of the Al-stabilized superconductor, aiming to demonstrate full-scale conductor fabrication, production of sufficient lengths, and mechanical performance that meets the required safety margins.

The full-scale conductor is very important. We will develop the full-scale conductor with sufficient length in the year 2025 which meets the requirements of CEPC.

Recommendations

- Develop a detailed plan for the construction and testing of a superconducting model coil, including demonstrations of cooling and excitation. Achieving this milestone is essential for progressing toward full-scale magnet construction.

Establishing a scaled model coil is really a necessary step before the processing of the detector magnet, and we will take this important process into consideration in our subsequent planning.

- Finalize the cooling system design based on the thermosiphon concept, with particular attention to the reliability and quality assurance of aluminum-pipe welding procedures during construction

We will optimize the design of the cooling system. While we have experience in welding small model coils, we have not yet tackled the welding of such a large number of pipes in a large-scale cooling structure. We plan to conduct verification experiments in the near future to ensure reliability and quality assurance.

Finding and comments on Draft v0.4.1

- The superconducting (SC) solenoid design for the CEPC Reference Detector Technical Design Report (Ref-TDR) has significantly progressed. Congraturations!
- The solenoid provides a central magnetic field of 3T (for $t\bar{t}$, Higgs, and W runs) and 2–3T (for Z runs), within an inner bore diameter of 7.07 m and a cryostat/yoke length of 9.06 m. As a fundamental number, the SC magnet stored energy (E) is 1.5 GJ with the coil mass (M) of 145 tons with E/M = ~ 10 kJ/kg. It is assembled with an iron yoke, helically assembled, also with muon detectors. The profile and uniformity of the solenoid magnetic field in the central tracker (TPC) region is expected to be approximately 7%. It would be OK, if the TPC may accept this field variation.
- The solenoid coil is composed with four layers coils wound with Al-stabilized superconductor, supported by an outer support cylinder made of Al-alloy and cooled by using a two-phase helium natural convection flow with a thermo-siphon scheme. This design concept has been well experienced and established with previous collider detector programs, such as the CERN-LHC CMS detector and others.
- The 'box-type Al-stabilized superconductor' with two step co-extrusion has been uniquely proposed, and the development is in progress. It is expected to successfully demonstrate the full-scale box-type conductor within 2025. It shall be a very important milestone and strongly encouraged. However, it is also important to keep backup solutions to be prepared for the box-type conductor development not to be successful.

Finding and comments on Draft v0.4.1

- The mechanical stress analysis is advanced. However, the results have not been clear enough and the mechanical safety design has not been clearly described. It would be very important to determine necessary mechanical strength of the Al-stabilized superconductor with the box-type design and to be consistent with the performance test results from the conductor development. It must be critically evaluated.
- The SC coil winding design with a four-layer coil is to be wound by using an 'inner coil winding technology', and it sounds reasonable and promising. The demonstration by using a dummy conductor has been successfully made in cooperation with industry. It needs to be recognized as a preparation step for a SC model coil to be developed and SC performance to be demonstrated.
- The quench protection and safety design is based on two technologies of 'partial energy extraction' by using an external dump resister and 'quench back' inductively induced by the external support cylinder, functioning a single-turn secondary circuit. On the other hand, an expected energy extraction fraction of $> 80\%$ may need to be confirmed or updated. If the coil temperature would be increased to ~ 60 K on average after switching off the circuit, a half of the stored energy might be already dumped in the coil. The energy extraction ration would be more reasonable with a level of $\sim 50\%$. The quench protection study may be further improved.

Recommendation on Draft v0.4.1

- Proceed the ‘box-type’ Al-stabilized superconductor as the highest priority, aiming to demonstrate full-scale conductor fabrication, and to verify the superconducting and mechanical performance that meets the required safety margins. It will be important to demonstrate a sufficiently continuous length, at least, enabling to realize a superconducting model coil to be fabricated and the superconducting magnet performance demonstration. In parallel, backup solutions shall be continued to prepare for the case of the ‘box-type’ not to be practical.
- Advance/improve the quench protection and safety study that reach a reasonable estimate for a balance of the coil temperature rise after the quench and the energy extraction ratio. It is a fundamental balance to be well understood.

ELECTRONICS

Findings

- The reference TDR provides a clear and accurate description of all on-detector and off-detector electronic systems required for the readout of the various detectors, along with their associated 17 requirements—many of which are critical to the overall experiment performance. Since the last committee meeting, several important decisions have been taken, most notably the adoption of full data transmission (streamed readout), which is now firmly established.
- The nine different ASICs, currently at various stages of development, are clearly summarized, with an assessment of their maturity ranging from level 2 (initial design) to level 4 (prototyped) on a 1-to-5 scale. Three of these are common service ASICs used for power distribution and data transmission. The required manpower for the ASIC developments and future steps is well detailed and appears realistic.
- The shared back-end architecture and power distribution scheme are also well described, building upon the solid experience gained from large-scale operational experiments such as JUNO.

Comments

•The committee is very impressed with the progress made and the thorough implementation of previous recommendations. In particular, the decision to adopt a data streaming readout is a major step forward, significantly impacting the ASIC architecture. The handling of data rates and the application of safety margins are well managed.

•The ASICs are well documented, and several key building blocks have already been successfully prototyped, demonstrating the strength and efficiency of the teams involved. The progress is remarkable; however, as the complexity of the chips increases, substantial work still lies ahead. It would be helpful for each ASIC to clearly identify the lead responsible person(s) and the contributors to the various blocks and development tasks.

•The responsible persons have been assigned for each chip.

•Data Link: FEDA, FEDI, OAT – Di Guo (CCNU)

•Power: PAL – Jia Wang (NPU)

•SiPM - SIPAC: Huaishen Li (IHEP)

•OTK – LATRIC: Xiongbo Yan (IHEP)

Comments

- Verification of the ASICs is critical, especially for large chips that include substantial digital logic (e.g., tracking ASICs). Verification should be conducted by individuals independent of the design teams and should use state-of-the-art tools and methodologies.
- Testing of ASICs can never be too extensive: it should involve not only the designers but also multiple user teams wherever possible. Chips should be characterized across a range of temperatures and supply voltages to detect weaknesses early. As larger volumes become available, systematic analysis of failing or underperforming chips (“bad chips”) will be essential.
    - **Part of the verification has been done during the design phase by the design team. However, more verification work should be done while lack of manpower**
    - **Independent verification work will be done during the test phase by independent teams, for which it is not so high-level tech required**
- From a stylistic standpoint, the SIPAC chip (common to three detectors) is extensively described within this chapter, while other ASICs are detailed within each detector’s respective section. For improved readability, it may be preferable to move the SIPAC description to the calorimeter section, retaining in the electronics chapter only a general overview of all ASICs and a detailed view of the shared service chips (e.g., for power and data transmission). For the front-end ASICs, detailed schematics could be reduced in favour of presenting more relevant simulation results, such as pulse shapes or noise versus input capacitance.
    - **We have done exactly as suggested.**
    - **SIPAC part has been moved into the ECAL chapter, and shrunk for the length and details, only the main specs and scheme were kept.**

Comments

- The back-end electronics are comprehensively described and benefit from the team's previous experience with large-scale systems. However, the availability of high-performance FPGAs could pose a risk. Maintaining a dual-source strategy for critical components would be a prudent mitigation measure.
  - **Yes, that is also our current idea. We have kept eyes on backup resources for the key components. Almost all of them have found extra vendors or substitutes.**
- Identify the teams responsible for testing each ASIC, ensuring they are different from the design teams. Bugs are often discovered late in development, and broader involvement in chip evaluation improves characterization and helps uncover potential weaknesses.
  - **See the answer for the comment 1.**
  - **We have assigned the teams and responsible persons for each chip.**
- Begin detector testing with available “sister chips” where feasible. This parallel approach can advance both detector and chip development and provide valuable benchmarks for comparison.
  - **This is the idea during previous R&D for detector prototypes, like for the ECAL.**
  - **We will follow this way for the future R&D for the early prototypes for sub-detectors. “Sister chips” (like the ROC chip series) will be evaluated to make the chip development in parallel (to some extent) with the detector R&D.**

Recommendations

- Minimize power dissipation at every stage. Each milliwatt of consumption should be justified by a specific performance requirement.
  - We are continuing optimize the scheme.
  - Currently we have several consideration:
    - Optimize the OTK detector design, so that the power may be saved.
    - Optimize the electronics design for HCAL, according to the new design from the detector side. Channels will be saved, and frontend will be reconsidered with less dynamic requirements.
- Proceed with system development in parallel with chip development. System-level issues can often be addressed early at the chip design stage if identified promptly.
  - We will keep that in mind.
  - Actually we already have a prototype design of the common backend board, which works well and has been verified. We will optimize the design for the following prototypes of sub-detector R&D.

Comments on Draft v0.4

- However, I regret that the overview of the ASICs has also been removed and it only figures as the "next steps" in section 11.10, squeezed in a table which is actually difficult to read. The previous version which was detailing the different ASICs, their number, number of channels, level of maturity, existence of a "sister chip"... was very important and helpful. As in many experiments, they are likely to be a corner stone of the project and they should not become stumble stones !
  - We have added this table in the Ref-TDR, to describe the maturity of all related ASICs and similar chips. The table can be found below:

Name	Application	Functionality	Maturity	Similar chips
FEDI	Common Elec	Data Link	2~3	lpGBT[17]
OAT	Common Elec	Optical	3~4	VTRx[42]
FEDA	Common Elec	Data Aggregation	2	lpGBT[17]
PAL	Common Elec	DC-DC	2	bPol[43]
Taichu	VTX	VTX-Stitching	2~3	MOSAIX[44]
TEPIX-TPC	TPC	Pixel TPC	3~4	Gridpix[45]
COFFEE	ITK	HVCMOS	3	MightyPix[46]
LATRIC	OTK	LGAD-TOF	2	ALTIROC[47]
SIPAC	SiPM ASIC	ECAL, HCAL, Muon	2~3	HGCROC[48]

TDAQ

Findings

- The TDAQ system is based on the full transmission of data from the front-end electronics to the back-end electronics (BEE), with the trigger operating at the BEE level. Data rates from each subsystem are provided for the different CEPC operational scenarios; however, the underlying assumptions behind these estimates should be discussed more explicitly in some cases.
- The TPC represents a special case due to its long drift time, and a more detailed discussion of the implications of this extended integration time is necessary.
- The first stage of the trigger is planned to operate on the BEE boards, generating trigger primitives from the calorimeter and muon systems, with the possible addition of primitives for a track trigger. The trigger architecture has evolved to include BEE-resident primitive algorithms alongside a three-layer L1 hardware system. The CEPC team has demonstrated that simple requirements on calorimeter and muon primitives effectively reduce background rates while preserving high efficiency for the primary physics processes of interest, addressing a key recommendation from the previous review.
- It was noted that some exploratory work on a fast-track trigger has been conducted, though no results were presented. A silicon-based fast track trigger remains of high interest, as it would complement calorimeter and muon primitives and provide stronger separation between collision and non-collision backgrounds.
- This review focuses primarily on the ZH production and low-luminosity Z-pole running planned for the first ~10 years of CEPC operations. Nevertheless, the overall TDAQ design appears appropriate for other planned running modes as well.
- The Ref-TDR chapter should first describe the proposed baseline trigger system before presenting proof-of-concept studies for the trigger primitive algorithms.

Comments

- The background event rate and event size are critical inputs to defining the TDAQ system dataflow requirements. Assumptions used should be explicitly stated and consistently referenced across all relevant chapters (some inconsistencies were noted in the current draft).

- >>The detail information for the event rate and event size are summarized in table 12.3 and 12.4. The event size is calculated based on the information from the electronic chapter, and the time windows for each sub-detector.

Table 12.3: Time windows for each subdetector and the event size calculation for both Higgs and Z mode. The "Full Data" is from Figure 11.1. The data size per bunch is derived by dividing the "Full Data" by the collision frequency, with the Higgs mode collision frequency being 1.34 MHz and the Z mode 12 MHz. The data size per event is obtained after accounting for the impact of the time windows of each sub-detector on individual events.

	VTX	ITK	OTK	TPC	ECAL	HCAL	Muon	Total
Time windows (ns)	223	53	53	34023	323	1023	123	
Higgs mode Full Data(Gbps)	2220.0	16.4	79.0	52.7	1440.0	975.8	<1	4784.9
Data size / bunch (kB)	207.1	1.5	7.4	4.9	134.3	91.0	<0.1	446.4
Data size / event (kB)	207.1	1.5	7.4	604.7	268.7	364.1	<0.1	1453.5
12.1MW Z mode Full Data(Gbps)	8900.0	25.8	130.7	47.8	1111.0	808.0	<1	11024.3
Data size / bunch (kB)	92.7	0.3	1.4	0.5	11.6	8.4	<0.1	114.8
Data size / event (kB)	370.8	0.3	1.4	244.5	57.9	126.3	<0.1	801.1
50MW Z mode Full Data(Gbps)	25700.0	79.4	399.0	150.0	3450.0	2574.0	<1	32353.4
Data size / bunch (kB)	81.6	0.3	1.3	0.5	10.9	8.2	<0.1	102.6
Data size / event (kB)	815.4	0.8	3.8	701.0	153.2	367.5	<0.1	2041.6

Table 12.4: Trigger rate estimation table for different run conditions. The physical event rate is introduced in Section 12.1.1.1. The detailed readout rates of each sub-detector are shown in Table 12.12.

Operation phase		**I**		**II**	**III**
Condition	**Higgs**	**Z (12.1 MW)**	**W**	**Z (50 MW)**	**$t\bar{t}$**
Non-empty bunch crossing rate(MHz)	1.34	12	6.5	39.4	0.17
Luminosity ($10^{34}/cm^2/s$)	8.3	26	26.7	95.2	0.8
Physical event rate (kHz)	0.5	10	1.1	40	5.7×10^{-2}
L1 triger rate (kHz)	50	120	65	400	2
DAQ readout rate (Gbyte/s)	49.0	72.8	-	-	-
HLT rate (kHz)	1	20	2	80	1
Raw event size (kbyte)	1453.5	801.1	1500	2042	1000
DAQ storage rate (Gbyte/s)	1.5	16	3	163	1

Comments

- The safety factors applied in system design should be made explicit, clearly motivated, and documented to allow for easy updates and assessment of their impact on different subsystems.
- >>A safety factor "1.5" is applied when estimating the event size, mentioned in section 11.2: "During the calculation, a safety factor of 1.5 was considered for the background rate.". Another safety factor "10" is applied when estimating the trigger efficiency, as mentioned in section 12.4.1: "For both the Higgs and the Z mode, each beam background event includes 10 bunch crossings, corresponding to a safety factor of 10.“
- Section 12.4 should be moved after Section 12.6 to improve the logical flow of the chapter.
- >>Done.

Recommendations

TDAQ

- Clearly motivate the data bandwidth requirements into the L1 trigger, between trigger layers, and specify the number of links needed. Provide details on the expected trigger primitives from each BEE type and the associated data volumes. Similarly, describe the output products of the local trigger layers and provide data bandwidth estimates into the global trigger layer.

- Update the design of the common trigger board—particularly the bandwidth and input link capacities from the BEEs—to reflect the information presented. Explain the rationale behind the estimated number of trigger boards required at each of the three L1 levels.

- >> These part is added in "resource estimation" section as following. In the resource estimation, the trigger primitives for ITK, OTK, ECAL and HCAL are cluster information, which includes cluster position, size, energy information and time information; The muon detector provides hit counting information, including hits number, hit position and timing information. For TPC detector participating in trigger further research is needed. Currently only preliminary estimates are made based on its' data volume. The estimation of global trigger part of each detector is based on the divisions of sector. All trigger primitives information is obtained from off detector electronics. Trigger primitive transmission to trigger system from back end electronics is based on 10Gbps line rate, 8Gbps bandwidth removing the encoding overhead of 8B/10B. In the Level-1 trigger system, 16 channels of optical will be used for connection with off-detector electronic boards or previous level trigger boards. Based on the data volume of trigger information which calculated based on background simulation of each detector, trigger optical links to each detector's sub-trigger and number of trigger boards can be estimated. In trigger system installation, one ATCA crate can install up to 10 trigger boards and at least one DCTD board. According to this calculation approach, a rough scale of trigger system was estimated as shown in table 12.5.

Table 12.5: L1 Trigger resource estimation table. The number in parentheses represents the resources required for track trigger additional, in which ITK, OTK and TPC will be used.

Detector	Area (m^2)	Modules	Elec. Board Num	Area/BE (m^2)	Modules/BE	Hit Rate(10^3Hz/cm^2) or cluster in BX	TP Bits	Trigger Board	ATCA Crate	DCTD Boards
TPC	–	–	32	–	–	–	–	(2)	(1)	(1)
ITK-Barrel	11.9	–	149	0.086	–	34.8	64 bits	(9)	(0)	(0)
ITK-EndCap	2×9.89	–	78	0.2	–	487	64 bits	(51)	(6)	(6)
OTK-Barrel	65	–	34	1.92	–	4.82	64 bits	(3)	(0)	(0)
OTK-EndCap	2×10	–	45	0.67	–	23.9	64 bits	(4)	(1)	(1)
ECAL-Barrel	–	480	60	–	8	1 cluster/module/BX	48 bits	8	1	1
ECAL-EndCap	–	224	28	–	8	1 cluster/module/BX	48 bits	4	1	1
HCAL-Barrel	–	640	346	–	2	1 cluster/module/BX	48 bits	22	2	2
HCAL-EndCap	–	128	192	–	1	1 cluster/module/BX	48 bits	12	2	2
Muon-Barrel	–	144	18	–	8	1 fiber/trigger/BE	–	1	0	0
Muon-EndCap	–	96	6	–	16	1 fiber/trigger/BE	–	1	1	1
Global Trigger	–	–	–	–	–	–	–	18+(12)	2+(2)	2+(2)
TCDS	–	–	–	–	–	–	–	1	1	1
Sum	–	–	–	–	–	–	–	67+(81)	10+(10)	10+(10)

Recommendations

- Provide a detailed description of how the TPC data stream will be handled, especially considering its long drift times.
- >>A new paragraph for the TPC data stream detail information is added in section 12.1.2. It can still utilize L1 to pack TPC data whatever all raw data need be read out with more than 30 kHz L1. Data is packed in blocks by multiple Trigger ID for parallel processing. TPC data is easily located via Trigger ID, enabling joint analysis with other detectors sharing the same trigger.
- Continue exploring the development of a fast-track trigger, emphasizing its potential to reduce background rates and ease the load on the HLT.
- >>A preliminary track trigger study is added in Section 12.4.2.1. The current results doesn't improvement the trigger selection, further study need be done in future.

Recommendations

- Demonstrate the necessity for RDMA technology in transferring data from the BEE to the HLT, including a justification based on system performance needs.

- >> Currently, CEPC's baseline design is to use the traditional TCP protocol for data transfer from the BEE to the HLT, while RDMA is primarily being considered as a research direction. This consideration is mainly based on the following points:

  - 1.RDMA supports direct memory access, significantly reducing CPU utilization during data transfer. This helps to overcome the performance bottlenecks of traditional protocols and meet the demands of future high-throughput data transmission (e.g., for high-luminosity Z mode).
  - 2.Validating RDMA on the existing readout electronics platform in advance can prevent large-scale hardware upgrades triggered by data volume growth, thereby lowering the cost and technical risks of future system upgrades.
  - 3.Applying RDMA in the high-level trigger system can reduce CPU load and interrupt overhead during data transmission, improve the efficiency of trigger algorithms, and lay the technical foundation for future one-to-many data distribution and real-time event assembly.

- In summary, although the current TCP-based solution can already meet present requirements, early research into RDMA is a forward-looking strategy that can meet the demands of future experiments for high-performance data transmission, aligning with the development trends of leading international particle physics projects.

Recommendations

- Describe the system’s strategy for handling data flow in the event of full buffers to avoid data loss or system instability.
- >> This added in 12.2.4. BEE should generate full signal when buffer full and feedback to TCDS, TCDS will mask the L1 signal until full or error signals cleared to avoid data overwriting in data packing buffer in DAQ readout.
- Evaluate whether the L1 trigger hierarchy could be simplified, for example by collapsing it into a multiplexer layer feeding directly into boards handling full global trigger primitives.
- >> Fast trigger and Gobal trigger are combined as one layer according to the suggestion, see the Fig12.2. Trigger primitive generation is divided into local and global two layers one reason is that it is restricted by common trigger board IO number and FPGA resources we can purchase. Structure maybe optimized with the development of FPGA IO and resources we can buy in the future.
- Categorize the event rates into physics signals (e.g., ZH production, two- and four-fermion processes, Bhabha scattering), gamma-gamma interactions, beam-related backgrounds. The first category aims at full trigger efficiency, the second one is potentially of some interest but with lower priority and the last one must be reduced as much as possible.
- >>In table 12.1 and 12.2, the physical processes are categorized into two group "high priority" and "low priority". All the gamma-gamma interactions are under "low priority".

Recommendations

TDAQ

- Analyze the beam background distributions as functions of energy, multiplicity, and polar/azimuthal angle to optimize background suppression algorithms. In particular, investigate the origin of background peaks such as the one observed at ~7 GeV in the ECAL endcap (Figure 12.10)

- >>The beam background energy deposition in the Endcap region is studied. The first figure below shows the average energy deposition on the ECal Endcap modules for the 10000 beam background events, the second and third plots show the average energy deposition for the Endcap cell (~1.5cmx1.5cmx40cm) in different theta (azimuthal angle) region. The smaller theta, the larger energy deposition. An angle dependent energy threshold will be implemented.

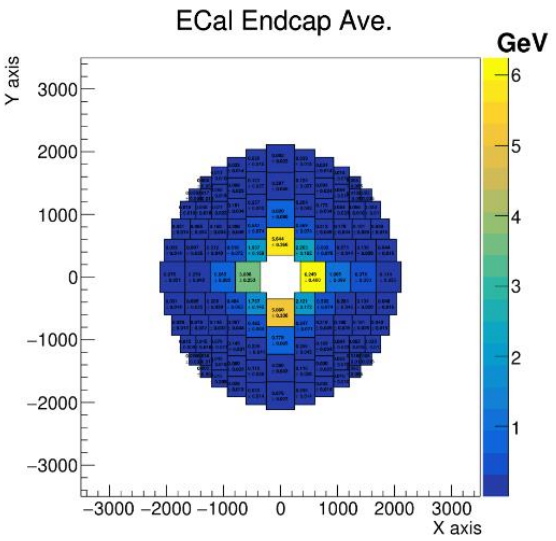

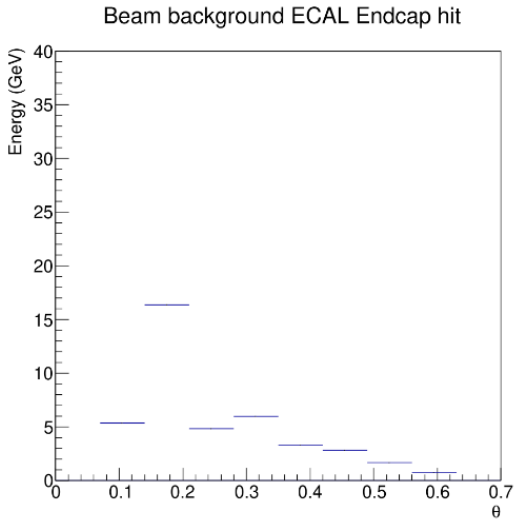

Comments from Bob on Draft v0.4

- It would help the reader to have stated early in the chapter the timelines associated with different decisions. For example, at lines 10835-10837 additional R&D is listed as being necessary. By when does this R&D need to be completed? Similar comment for lines 10875-10876. This arises again at lines 10944-10947. There is some discussion of timelines at the end of the chapter (lines 11836-11838); I suggest this timeline is referred to earlier.
  - This version of ref-TDR is aiming at Higgs and low lumi-Z modes. Current there is no technical bottleneck for CEPC Phase-I TDAQ. High lumi-Z mode is Phase-II of CEPC. The requirement of technical for High lumi-Z is not included in this version.
- In fact, it might be good to start the chapter with the summary and then give the details.
  - Add a summary section in overview

Comments from Bob on Draft v0.4

Some minor things I noticed as I read:

- 10849-10852: not sure what is being said here
- ->In the high luminosity Z mode, the data volume of the detector will be significantly increased. The \gls{TDAQ} system should have scalability to cope with such situations.
- 10890-10893: not sure what is being said here

->Most of the \gls{L1} trigger algorithm will be running on \gls{FPGA} farm, which has the advantage of low latency and real time. As the principle of trigger is to keep all the good events and reduce the background events to acceptable level of \gls{DAQ} readout, it is challenging to maintain the data purity.

- 10897-10900: repeated sentence.
- Deleted the repeat sentence
- 10916-10917: trails = tracks?
- trails -> tracks
- 10922-10924: not sure what is being said here
- ->The combination of these physical objects can be used to reconstruct the particle flow object and further suppress the background process.
- 11090-11091: meaning unclear
- Global trigger resource allocations for each subsystem employ sector-based segmentation as the foundational calculation method. For global track trigger, Calorimeter track finding, and Global trigger, 60° will be defined as a sector. For the energy trigger of the calorimeter, 120° will be defined as a sector.
- 11813-11814: text is garbled, not clear what is meant
- ->Following the recent update results of sub-detector design and simulation, significant progress in the technical development of the \gls{TDAQ} and online systems has been achieved.

SOFTWARE AND COMPUTING

Findings

- The review team acknowledges the very good progress made in software and computing since the last report. Almost all previous recommendations have been successfully addressed by the collaboration. The current status and advancements are thoroughly documented in the Ref-TDR and were presented and discussed during a dedicated session at this review. Overall, the Offline Software and Computing activities are in a strong position, the outlined approach appears highly feasible, and no significant challenges or showstoppers have been identified.
- The offline software, CEPCSW, is based on the international Key4hep project, which is used by all future collider projects. CEPC is making significant and well-aligned contributions to this effort within the global community. In terms of computing, CEPC leverages established tools and methodologies developed for the LHC. The current computing model follows the traditional Tier structure, though a transition to a more efficient model is envisaged, aligned with broader community developments.
- A detailed simulation model of the reference detector has been implemented. For track reconstruction, the collaboration is currently adapting tools and algorithms from the linear collider community while also developing more advanced techniques. A new particle flow algorithm, CyberPFA, has been developed, particularly to meet the challenges posed by the novel crystal ECAL design. This builds on prior work from the HCal side and has been successfully integrated into CyberPFA. The full simulation and reconstruction framework has been employed to produce a comprehensive set of technical performance plots, demonstrating that the detector concept, combined with sophisticated algorithms, can meet the required physics performance targets.
- The offline software has also been used to estimate the computing needs, based on reasonable— though not highly refined—assumptions regarding data rates, data volumes, processing schedules, and methodologies. However, the estimates also assume optimistic developments in CPU performance and cost trends over the next decade.

Comments

- The corresponding Ref-TDR chapter would benefit from some revisions: reducing the length of more general descriptive sections and expanding technical details where appropriate.

  The total number of pages has been reduced from 62 to 41, plus an additional 4 pages for citations.

- Some important aspects of the planned computing model remain insufficiently detailed, such as the structure for user analyses, data distribution strategies, open data policies, and long-term data preservation plans.

  Structure for user analyses, data distribution strategies:

Line 1064-1071: An efficient data distribution strategy within the data model is essential for optimizing data storage, access, and processing. Raw data will reside in central storage, while reconstructed data (RecData), simulation data (SimData), and analysis data (AnaData) will be distributed across Tier-1 storage. These datasets will be accessible on demand through a tiered storage and caching system, ensuring streamlined availability for various sites. A progressive reduction of the data format for user analysis, coupled with corresponding analysis facilities in \gls{Grid} and non-\gls{Grid} resources, creates a robust structure that enables fast and reliable user analyses.

Open data policies: A new section of 13.8 Open data was added.

Long-term data preservation plans: A new section of 13.9 Long term data preservation was added.

- The development of CyberPFA is a significant achievement and positions the collaboration as a leader in custom in-house algorithm development. However, the degree of reliance on existing tools like PandoraPFA and ArborPFA needs to be better explained and justified.

Line 533-536: The experience of clustering in high granularity calorimeter and integrating track and calorimeter information from \pandorapfa and Arbor are also adopted in \cyberpfa for the reconstruction in traditional high granularity \gls{HCAL} and optimal performance.

Comments

- While the event data model (EDM4hep) is well established, more detailed data formats for reduced, compact data levels (e.g., various stages of AODs) are not yet clearly defined.

Line 981-984:

\item AnaData (analysis data): which is a summary of the reconstructed event, and contains sufficient information for common analyses

\item TagData (event tag): summary of some general features of the event, allowing rapid access to the events and performing fast selection

Line 988-990:

AnaData and TagData are expected to be relatively smaller in scale compared to RecData. Given their importance for data analysis, they will be defined as soon as event-level reconstruction, following data reconstruction in sub-detectors, becomes available.

Comments

- The costs associated with the required computing infrastructure—such as whether a new data center will be necessary—are not discussed in the Ref-TDR.

Described in 13.10.4 Smart data center infrastructure

- While future technologies such as quantum computing, machine learning, and AI are mentioned, their potential roles and the motivation for pursuing them should be more clearly articulated, with better-defined staging scenarios

Line 723-736:

The trend in computing hardware is shifting toward increased CPU cores and more diverse architectures, including \gls{GPU}, FPGAs, and other accelerators. Machine learning plays a crucial role in high-energy physics experiments. Consequently, the development of software capable of efficiently handling simultaneous computations and leveraging machine learning techniques to enhance data processing and analysis has become an increasingly important topic.During Z-pole operation at CEPC, computing demands are expected to reach the exabyte scale, posing technical challenges comparable to those encountered at the High-Luminosity Large Hadron Collider. Advances in artificial intelligence, along with the integration of concurrent and heterogeneous computing, will form the operational backbone of future collider experiments. Meanwhile, quantum computing and its associated algorithmic frameworks present a potential paradigm shift in addressing these challenges, offering a promising—though ambitious—solution for the CEPC initiative.This section will present relevant research efforts exploring these advancements.

Recommendations

- Further develop and consolidate the detailed simulation model and reconstruction framework, with particular attention to:
  - Adding realistic estimates for detector imperfections, such as gaps or insensitive material from cables and services, to the simulation model.

    Line 163-167:

    \ddhep can also be used to represent more realistic geometry, rather than idealized models, by integrating alignment and calibration data. Misalignment corrections can be applied to reflect actual detector shifts, and calibration constants are included to ensure accurate detector responses. By incorporating these elements, DD4hep offers a comprehensive and precise detector description for the experiment.
  - Performing detailed studies of the CyberPFA performance, including jet energy resolution for light-quark dijet events, single particle responses, neutral hadrons, and neutrino energy measurements in b-decays.

    presented in Chapter 15
  - Studying the impact of misalignment on tracking performance.

    discussed in Chapter 15
- Develop a systematic performance monitoring framework, organized around a set of benchmark figures and analyses that qualify simulation and reconstruction quality. Each sub-detector should define its own "detector performance" plots, while a standard set of global physics performance plots should be maintained to validate software improvements.

  Line 217-219:

\item Release validation: Large-scale data production is manually triggered using predefined workflows, which are submitted to local or distributed computing systems. Key physical quantities are then compared against standard distributions, providing a clear reference for evaluating detector performance.

Recommendations

- Once consolidated, establish a clear reference for detector performance within the RefTDR, ensuring that future detector and physics performance studies use consistent versions and conditions (e.g., ensuring that jet resolution and b-tagging results are presented with the same software version and setup).

  Performance studies will be conducted using a fixed software release, as agreed upon with the physics group.

- Develop a more detailed and phased estimate of computing needs during the R&D and preparation phases, for example by organizing a sequence of increasingly challenging "data challenges." These would also serve as benchmarks for assessing the maturity of the offline software and computing infrastructure.

  Line 1023-1027: The allocation of computational and storage resources is divided into three distinct phases: 2\% during the TDR phase, 10\% during the construction phase, and 100\% during the data-taking phase. The detailed estimate of computing resources will be obtained through a series of increasingly complex data challenges, tailored specifically for the experiment.

Comments on Draft v0.4.1

- The Offline Software and Computing section of the TDR has been significantly improved wrt. version from the April review meeting at IHEP. Manyn of the comments have been well addressed, e.g. the overall length is reduced with replacing more general sections with technical descriptions, open data policies and long term data preservation plans have been added, the relation of CyberPFA to PandoraPFA is clarified.

- The CEPC Software and Computing group has also started to address the recommendations made in the previous review, e.g. by developing a more detailed and phased computing resource needs and the planing of dedicated computing challenges to monitor the progeress.

- A detailed data challenge plan has been incorporated into Section 13.6.2, spanning lines 1010 to 1026.

  "Detailed estimates of computing resource requirements will be obtained through a series of Data Challenges—large-scale Monte Carlo productions designed to validate computational needs before building the final system. These challenges will be conducted in multiple rounds, each increasing in complexity and data volume to more accurately simulate future CEPC operational conditions. Early stages will focus on prototype tests of offline software, profiling CPU, memory and storage demands for core algorithms, followed by full-chain processing from simulation to reconstruction, with particular emphasis on bottleneck and performance of key workflows. As the Data Challenges progress, later rounds will emphasize the generation of approximately 1 million Higgs events, complemented by inclusive Monte Carlo datasets that simulate one month of low-luminosity Z data collection. Those rounds will incorporate Grid computing integration, significantly enhancing the realism of both data processing workflows and analysis pipelines.

  The final phase of the program will feature collaborative efforts with the CEPC international sites, coordinated through a Common Computing Readiness Test. This structured approach ensures comprehensive validation of the computing model, overall operational readiness, paving the way for the full-scale deployment of the CEPC. "

- At the same time a number of recommendations have not yet been addressed, e.g. performing detailed studies of the CyberPFA performance, including jet energy resolution for light-quark dijet events etc. We encourage the group to continue to pursue these recommendations, well aware that not all will be possible before handing in the TDR.

- We've already started working on this. If everything goes smoothly, we expect to have results within two weeks.

MECHANICAL INTEGRATION

Findings

- Significant progress has been made since the last review in the mechanical design of the CEPC reference detector. The weight and boundary dimensions of each sub-detector are now well defined in the Ref-TDR. Clearances between sub-detectors are typically around 10 mm, which appears adequate to ensure a seamless installation sequence. However, in the critical interface between the integrated beam-pipe/vertex detector assembly and the ITK, the clearance is reduced to just 2 mm.
- The issue of sagging of the magnet yoke under its own weight has been effectively addressed. The introduction of end-flanges satisfactorily mitigates the problem, reducing the sagging from about 13 mm to within the required limit of less than 1 mm.
- The installation sequence has been carefully developed. The core shaft designed for the installation of the barrel HCAL and ECAL detectors appears adequate, as does the cantilever system proposed for installing the TPC, ITK, and beam-pipe assembly (including the Vertex and LumiCal detectors). The animations presented clearly illustrated the feasibility and logic of the installation process.

Comments

- The mechanical connection structures between sub-detectors are well designed, considering the specific requirements of each system. However, the methods by which these structures will achieve the precise alignment of the sub-detectors are only briefly described in the current Ref- TDR. Reference is made to an alignment control network that would provide positional benchmarks, but further details would strengthen the documentation.

Further details are to be looked into.

- Significant progress has also been made in designing the auxiliary facilities, which include the air-conditioning system for the experimental hall, gas and cooling systems for the various sub-detectors, power distribution and electronics systems, the cryogenic system for the superconducting magnet, and the hydraulic pump station used to move the detector to the collision point.

Yes, but the design of the ground floor hall is still missing and is planned to be carried out and implemented in the subsequent work.

Recommendations

- Further refine the routing plans for cables and services, especially in the critical interface areas between sub-detectors and through the barrel-to-endcap transitions to the outside of the detector and the auxiliary facilities.

  Work in progress.

- Pay particular attention to the air-cooling and service routing for the vertex detector, where space within the beam-pipe assembly is extremely limited. It is essential to verify that sufficient space is available to ensure the proper functionality of the air-cooling system, without compromising reliability or maintenance access.

  Work in progress.

- Regarding refrigerant choice for the other sub-detectors:
  - Supercritical CO_2 (sCO_2) could be considered as an alternative to water. As a single-phase refrigerant, it is user-friendly for complex, multi-branch systems. Like water, it is non-toxic, non-flammable, and readily available; unlike water, it is dielectric and harmless to electronics in case of leaks. While sCO_2 brings operational advantages, these must be weighed against some disadvantages (see appendix for details).
  - Boiling CO_2 (subcritical, operating around 20–25 ° C) is also simpler than twophase CO_2 systems, which require more complex design, maintenance, and expert operation. Thus, unless two-phase cooling is clearly necessary, a simple and efficient single-phase refrigerant (such as water or supercritical CO_2) is preferable

  Work in progress.

Comments in backup

Detailed Considerations on the Advantages and Disadvantages of a Refrigeration System Based on Supercritical CO_2 (sCO_2) Compared to Water.

Advantages of sCO_2 Refrigeration:

- sCO_2 is fully dielectric, making it inherently safer for use near sensitive electronics.
- sCO_2 requires much smaller piping for the same flow rates due to its lower viscosity and higher operating pressure.
- It has a higher heat transfer coefficient, provided that operational conditions (temperature and pressure) are well optimized.
- The high fluid pressure allows for larger acceptable pressure drops in the heat exchanger (e.g., in the detector stave's tubes). With optimized heat exchanger design, it is theoretically possible to induce the necessary pressure drops to maintain nearly isothermal conditions—achieving single-phase flow with the same inlet and outlet temperatures while efficiently removing heat.
- Experience shows that low-pressure circuits tend to develop leaks over time due to lower quality construction standards, while high-pressure systems, requiring stricter quality controls, are more robust. This leads to lower long-term maintenance costs (both financial and operational).

Disadvantages of sCO_2 Refrigeration:

- High-pressure systems are generally estimated to be 15–20% more expensive than equivalent low-pressure systems.
- Operation at 30–35 °C might impact surrounding systems and needs to be considered during integration.
- A dedicated pressure control component ("bladder" or similar device) is required to maintain stable system pressure.
- Depending on the system volume, there are potential safety issues (especially personnel safety) associated with storing large quantities of CO_2 in confined underground spaces.
- The combined effects of all parameters (temperature, pressure, flow rates) on the thermal fluidic behaviour of supercritical CO_2 are not yet fully understood. However, significant research and development work in this area is currently ongoing

Comments on Draft v0.4.1

- However, unless I have overlooked something, the two main recommendations we made in April the 2nd review in April have been addressed yet:
  - Refine the routing plans for cables and services, especially in the critical interface areas between sub-detectors and through the barrel-to-endcap transitions to the outside of the detector and the auxiliary facilities.
  - Pay particular attention to the air-cooling and service routing for the vertex detector, where space within the beam-pipe assembly is extremely limited. It is essential to verify that sufficient space is available to ensure the proper functionality of the air-cooling system, without compromising reliability or maintenance access.
- They might not have had the time to do so yet, but I regret that in the to-do list at the beginning of the document it only says:
  - Mechanics and integration is mostly done, but requires improvements to the text, and cross references, and minor changes to increase plot sizes. No new studies are planned to be added.
- It would be important that they take at least note of the comment and indicate how they intend to address the topic in the future. If they could make at least an estimation that routing and cables and services works on paper, it would already be good.
- I have no line comments to provide yet and would prefer to do so only at a later stage, when the document has undergone further editing.

DETECTOR PEREORMANCE

Findings

Although further improvements are possible and recommended, the collaboration's response to the previous evaluation has been excellent and deserves recognition. The detector software, particularly the simulation component, now enables comprehensive studies of detector performance and physics benchmarks. Several design decisions have been made based on both detector and physics performance criteria. This progress has allowed the definition of a baseline detector concept. While still perfectible and requiring further detailed investigation, this is a significant and commendable step forward. The scope of physics performance studies has broadened considerably since the last assessment. The range of channels explored and the methodologies employed respond well to previous recommendations and collectively address key detector areas and primary physics topics.

Comments

- The Ref-TDR text could be improved and shortened by presenting certain aspects (e.g., particle identification, jet studies) more concisely, while still ensuring that the algorithms are described clearly and transparently. *shortened and reorganized*
- Many additional physics analyses are planned. Their presentation and motivation should be aligned with the main purpose of this document: demonstrating the feasibility and physics potential of the reference detector. *several more analyses implemented and included since last review*
- Algorithms for particle identification, jet tagging, etc., are mentioned in multiple places and are still evolving. A systematic approach should be adopted to define and refer to these algorithms consistently across the document. *restructured, and referencing properly done.*

Recommendations

- The studies encompass both physics benchmarks and detector performance metrics. A clearer distinction between these two aspects would be beneficial. The editorial team is encouraged to organize the content into:
  - Sub-detector technical performance — technical performance figures (used for sub-detector configuration decisions) should be placed in the relevant sub-detector chapters.
    - *Single photon reconstruction efficiency and resolutions now only shown in ECAL chapter*
    - *Tracker impact parameters now appear only in Vertex chapter*
  - Physics-related performance — to demonstrate baseline detector capabilities for physics analyses (e.g., particle identification, global variables like ETmiss), and to present the physics analyses themselves. This should be the main focus of the performance chapter.
    - *Full system tracking, PID (TPC+TOF) are also in Silicon chapter: duplicated plots removed in perf. chapter*
- The physics benchmarks listed in Table 15.3 are intended to demonstrate the performance of the reference detector. Each listed study should be discussed explicitly, explaining the role of the detector performance in achieving the result. Currently, only a subset (e.g., Higgs recoil mass, Higgs branching ratios, weak mixing angle from $Z \to \mu\mu$) are covered. Other channels (exotic Higgs decays, LLPs, CVP in D-meson decays) should also be summarized, possibly in a summary table. *More channels (being) added*
- The technical improvements planned for more detailed simulation (noise, event overlap, misalignments, calibration effects) should be pursued, and their impact on physics performance carefully demonstrated.
  - *Noise checked (negligible), event overlap evaluated on tracking (5% worse resolution)*
    Studies of event overlap in calo, misalignment effects underway

Recommendations

Several specific technical issues should be clarified and potentially improved:

- The photon efficiency behaviour around E = 1 GeV appears unusual and should be either justified or corrected, as it could impact EM/hadronic separation in PFA and influence missing energy and mass resolution. *discussed in ECAL chapter*
- Jet energy resolution for light quarks should be studied more systematically and used as a benchmark metric. *Ongoing*
- Missing energy reconstruction should be further investigated, particularly in b- and c-jet events with tagged leptons and in BSM channels with large ETmiss. *done, a section on missing E/M added*
- (Longer term) Tracking performance should be tested in exotic scenarios, such as long-lived particles. *Beyond TDR*
- (If possible) Include photon conversions in tracking studies as a material probe and describe their treatment in PFA. *added material budget plot and conversion rate vs. cos(theta)*
- Particle identification needs further organization and development:
  - Currently, simple cuts are applied; more sophisticated algorithms (including ML-based methods) should be considered, balancing the ambition against available time and resources. A simpler multivariate approach could serve as an intermediate step. *XGBoost is default now*
  - Different working points ("tight" for high purity, "loose" for high efficiency) should be defined and used consistently across analyses (e.g., Figure 15.7, where a 90% WP for muon/electron ID is mentioned). Coherence with PFA must be ensured (avoiding double-counting residual energy, etc.) *BEST WP used now*

Recommendations

- The description of jet flavor identification needs to be streamlined. Currently, information is dispersed across sections (vertexing, tracking, PFA). A concise but complete description should be provided in one place *restructured*
  - A brief overview of standard Jet Flavour Tagging (JFT) is given in Section15.2.6, while Jet Origin Identification (JOI) is discussed in 15.2.7. However, it is unclear what performance gains are achieved by moving from JFT to JOI. *JFT vs JOI shown for b/c tagging eff and mis-id rates*
  - Benchmark comparisons (b/c-tagging efficiency versus misidentification rates at Z-pole and ZH 240 GeV) should be provided to evaluate performance systematically.
- The offline software environment is evolving rapidly. Performance studies should be conducted with synchronized and version-controlled frameworks, especially as CyberPFA depends critically on tracking, particle ID, calibration, and alignment inputs. *yes*
- A centralized database tracking the produced samples and their statistics should be maintained and updated (extending Table 15.4). Technical samples (e.g., single electrons, muons, decaying kaons for PFA studies) should be included and documented similarly for use in detector performance validation.

  a centralized database created and maintained with IHEP gitlab service (in CEPCSW code repository)

Recommendations

- Longer-Term Considerations (for post-TDR development)
  - Consider a dedicated chapter for jet flavour tagging, especially given the comprehensive nature of JOI (which involves many sub-detectors). Comparative studies between "ideal" and "compromised" performance would also help derive systematic uncertainties in the AI-based approach.
  - The confusion matrix (Fig. 15.22) suggests JOI could distinguish quarks from antiquarks. If validated, this could significantly improve flavour-specific AFB measurements. Physics benchmarks involving b/c-quark AFB (or even strange quarks) should be added if feasible.
  - Organizing "data challenges," as mentioned in the "Offline Software and Computing" section, could be valuable. These would serve both as benchmarks for detector performance and stress tests for computing models (through massive production, analysis, and quality checks)

Plan discussed to have another round of data production with a final TDR SW release in July-September

* based on detector design/geometry in June 15
* TDR SW release June 30 for internal test
* SW validation/fixes by July 30 - final TDR release
* August 1st - data production ~ 1 month
* all results updated in September

Comments on Draft v0.4.1

- The particle ID section 15.1 are now readable and well structured It would be nice if the section 15.1 ends up with a conclusion summarizing the salient performance features observed in these studies. I suggest a table of this type.

Particle Id.	Physics channel/sample considered	Performance exemple
Missing Energy	e+e-→HZ, $Z \rightarrow \mu\mu$, ee or qq $H \rightarrow ZZ* \rightarrow 4\nu$	deltaM ($Z \rightarrow \mu\mu$)=0.288 GeV deltaM ($Z \rightarrow$ ee)=0.40 GeV
Jets JOI	$\nu\nu.H$ production with $H \rightarrow$ qq and Ecm= 240 GeV	b-jet tagging efficiency of 95%with a misidentification rate of only 0.1% for light quark jets. ….

Comments on Draft v0.4.1

- - The physics benchmarks in section 15.2 should be listed by physics domain and in the same order as introduced in table 15.3
- - in table 15.3 W fusion appears out of order (the domain is “Higgs”). Maybe move it up together with “Higgs”.
- - 15.2 please make sure that each analysis presented have 1-2 phrases at the end to compare with a reference analysis (for instance present state of the art, limits from LHC or previous LEP results etc) This exists in some places but not everywhere.
- -This is not necessarily for this document, but on a few benchmarks items (MHiggs, MTop etc.) it would be good to have a direct comparison with FCCee studies. (and good answers if significant differences are observed)
- - Table 15.18: maybe having the cell limits would help readability?
- -Figure 15.33 : are the contours right? They seem to be confined at the right of the figure and are not readable.
- - The section 15.3 : I suggest to move the subsection 15.3.4 as a part of the final section, to be renamed as “Summary and future plans”.
- - I suggest to rename the section 15.3 as: “Further performance aspects”
- -I suggest a proof reading, there are a few editorial minute errors left in the text. (make the references uniform etc.) But in general the text is OK.

OVERALL CONSTRUCTION COST AND TIMELINE

Findings

- The cost estimation is provided as an ancillary table outside the Ref-TDR, following a standard Work Breakdown Structure (WBS). Only summary tables for the baseline detector option are included within the TDR text itself. Costs are primarily based on raw material prices (by volume, weight, or area), projected over the next 5 to 10 years, and multiplied by a fabrication factor.
- Currently, only a very rough timeline for detector construction is presented in Chapter 16 of the TDR.

Comments (1)

- For future, more informed cost reviews, it would be beneficial to provide the full WBS information, with a breakdown of:
  - Raw material costs
  - Production costs (including fabrication losses)
  - Labour costs
  - Integration costs
- Additionally, for each item, the following should be clearly specified:
  - Unit description (clearly linked to the detector design)
  - Unit cost (in original currency)
  - Basis of the estimate (e.g., vendor quote, internal prototype, previous projects, catalogue pricing)
  - Quantity required for the detector
  - Quantity including yield loss
  - Total quantity and total cost
- It should be explicitly stated whether the current costs include allowances for yield loss.
- A structured, consistent table format for each major cost item would greatly improve clarity and traceability.
- We plan for an internal cost review for each system in the second half of this year, with all above suggestions included. An international cost review is under consideration.

Comments (2)

- Concerning computing costs: while the extrapolations appear reasonable, the model could be further refined by considering data size, number of re-processing, number of data copies, and data accumulation schedules. Even a small additional effort to refine or document these factors would be valuable.
- The projections for hardware performance and price evolution over 10 years seem somewhat optimistic, as they combine assumptions of improved CPU performance per core with reductions in cost per core.
- The physics group and the offline group will work together to improve the estimation of data size and requirement of data processing. The extrapolation model will be further refined by analyzing price trends.

- Regarding the detector construction timeline, the information currently provided is too limited to allow for a meaningful assessment.
- A detailed timeline will be worked out in the detector EDR stage.

ECAL BGO Crystals

- The cost of BGO crystals significantly impacts the overall budget. The table presented dates back to 2019. We recommend engaging with multiple vendors to ensure the required quality, production rate (given the enormous volume), and lowest possible price.
- Before and after the review, we visited three suppliers of BGO.
  - SIC can produce BGO crystals of 1.5x1.5x40 (up to a meter) cm^3 by modified Bridgman method.
  - Xiamen Tungsten can produce BGO crystals of 8" x 3" by Kyropoulos method with possible significant reduction of cost compared with Bridgman method. They are working on longer (40 cm) crystals.
  - Boya can produce BGO crystals of 3" x 8" by Czochralski method while the cost is similar to Bridgman. They also plan to try Kyropoulos method.
  - **Action: collaborate with Xiamen Tungsten and Boya developing new methods**
- We also visited the research institute of the Aluminum Corporation of China (Chinalco) and its subsidiary, Yunnan Chihong Germanium International Co., Ltd.
  - Production capacity fully meets CEPC's requirement (~50 ton GeO_2)
  - **GeO_2 price increased by a factor of two since 2023, hard to predict the future trend**
  - **Action: potential collaboration with Chinalco through a high-level channel.**

SiPM Packaging Costs

- The cost of packaging could be as high as 50% or more. It should be clarified whether packaging costs are included in the quoted SiPM price, and this should be explicitly reflected in the WBS. The current estimate of 1.25 CHF per channel may be optimistic.
  - TAO uses SiPM 6×12 mm^2, 8 times larger than CEPC SiPM 3×3 mm^2
  - Assuming the cost packaging for CEPC is 50%, and for TAO is 25%, the new estimation is 20 RMB/piece, twice of our expectation.
  - Obtained new quotes from three suppliers, two of them below 20 RMB/piece including Hamamatsu. Further reduction expected in the next 5-10 years.

	TAO	Extrapolated to CEPC
Material	10 RMB	10 RMB
Packaging	3 RMB	10 RMB

Price of SiPM per 3×3 mm^2 based on TAO's experience

HCAL Cost Estimates

- Currently, the lowest informal offer is used for the cost of glass plates. Until it is confirmed that the lowest bidder meets the required specifications, it would be more prudent to use the average of the three quotes.
- The average price is 0.8 CHF/cc, 40% higher than our expectation (~0.5 CHF/cc). We will continue working with the three suppliers, to investigate their difference and to verify if the lowest price is reasonable.
- Additionally, the cost estimate assumes one SiPM per glass plate, whereas the detector design currently requires four SiPMs per plate for viability.
- In the new version of the TDR, the baseline design has been changed to one SiPM per glass plate.
- Some cost uncertainty reflecting the outcome of ongoing R&D should be included.
- If taking the difference between suppliers, the cost uncertainty is 40%, mainly coming from raw materials, the estimated yield and manufacturing procedure since it is a new material.

Muon Detector Electronics

- The cost book reports 43,000 ASICs, 43,000 FEE units, and 43,000 Readout FEE units. However, the readout architecture has recently been updated to a three-stage system, and the number of FEE boards (uFEBs) should be significantly lower than the number of SiPM channels. The cost estimate should be updated to reflect this new architecture.
- Additionally, the TDR mentions the need for 72 Management Boards for slow control and DAQ interfacing—these boards are currently missing from the cost book and should be added.
- The cost estimation including has already converted the total cost into the cost per single channel. Management boards are part of the on-detector FEE. The recent updates of the readout architecture, e.g. number of management boards from 72 to 80 are being incorporated into TDR and with be used to reevaluate the cost.

Magnet Cost Comparison

- The TDR quotes a magnet cost of about 22 MCHF, compared to around 130 MCHF for the more complex ILD system (which includes the yoke). A cross-check should be performed to understand and justify the difference between these two estimates.
- An internal review of the magnet design was organized on May 16. A detailed comparison with ILD will be done afterwards and a dedicated internal cost review is foreseen.

TPC Cost Comparison

- Similarly, the TPC cost is estimated at 5 MCHF, whereas the ILD TPC estimate was 36 MCHF. This discrepancy should be investigated and explained.
  - It seems that 36 MCHF is the sum of two options (Micromegas and GEM) in ILD. If only compare Micromegas, the difference between CEPC and ILD is not that large. Detailed comparisons are ongoing.
  - TPC cost (kCHF) in CEPC : 5223 + 1094 = 6317 (6.3 MCHF)
    - Electronics / Cost_total = 47.5%
  - TPC cost (kCHF) in ILD : 15360 (15.4 MCHF) using Micromegas
    - Electronics / Cost_total =57.2%
  - TPC cost (kCHF) in ILD : 19070 (19.1 MCHF) using GEM
    - Electronics / Cost_total = 46.5%@GEM